Cell Metabolism

Article

Obesity intensifies sex-specific interferon signaling to selectively worsen central nervous system autoimmunity in females

Graphical abstract

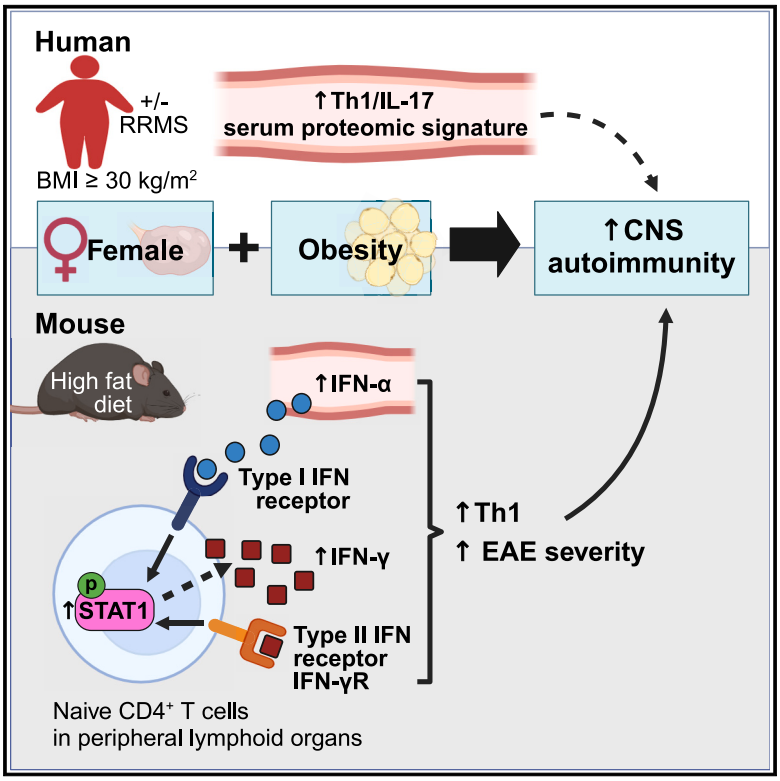

Highlights

- In women, obesity induces a pro-inflammatory Th1 serum protein signature
- In female mice, obesity promotes Th1 inflammation and worsens CNS autoimmunity in EAE
- Obesity increases serum IFN-α level and IFN-γ/STAT1 signaling in female CD4⁺ T cells
- Obesity exacerbates EAE in females through type I IFN signaling in T cells

Authors

Brendan Cordeiro, Jeeyoon Jennifer Ahn, Saurabh Gawde, ..., Daniel A. Winer, Robert C. Axtell, Shannon E. Dunn

Correspondence

bob-axtell@omrf.org (R.C.A.), shannon.dunn@utoronto.ca (S.E.D.)

In brief

Mechanisms by which obesity and female sex synergize to facilitate CNS autoimmunity remain elusive. Cordeiro and Ahn et al. reveal a female-specific effect of obesity in triggering Th1 inflammatory signatures in humans and augmenting IFN-γ/STAT1 signaling in mouse CD4⁺ T cells through type I IFN signaling, thereby exacerbating CNS autoimmunity.

Cordeiro et al., 2024, Cell Metabolism *36*, 1–17
October 1, 2024 Crown Copyright © 2024 Published by Elsevier Inc.
https://doi.org/10.1016/j.cmet.2024.07.017

CellPress

Please cite this article in press as: Cordeiro et al., Obesity intensifies sex-specific interferon signaling to selectively worsen central nervous system autoimmunity in females, Cell Metabolism (2024), https://doi.org/10.1016/j.cmet.2024.07.017

Cell Metabolism

CellPress
OPEN ACCESS

Article

Obesity intensifies sex-specific interferon signaling to selectively worsen central nervous system autoimmunity in females

Brendan Cordeiro,[1,14] Jeeyoon Jennifer Ahn,[2,14,15] Saurabh Gawde,[3,4] Carmen Ucciferri,[2] Nuria Alvarez-Sanchez,[1] Xavier S. Revelo,[5] Natalie Stickle,[6] Kaylea Massey,[3] David G. Brooks,[2,7] Joel M. Guthridge,[3] Gabriel Pardo,[3,8] Daniel A. Winer,[2,9,12,13] Robert C. Axtell,[3,4,*] and Shannon E. Dunn[2,10,11,16,*]

[1]Keenan Research Centre for Biomedical Science of St. Michael's Hospital, Toronto, ON M5B 1W8, Canada
[2]Department of Immunology, University of Toronto, Toronto, ON M5S 1A8, Canada
[3]Arthritis and Clinical Immunology Research Program, Oklahoma Medical Research Foundation, Oklahoma City, OK 73104, USA
[4]Department of Microbiology and Immunology, Oklahoma University Health Science Center, Oklahoma City, OK 73104, USA
[5]Department of Integrative Biology and Physiology, University of Minnesota, Minneapolis, MN 55455, USA
[6]Bioinformatics and High Performance Computing Core, University Health Network, Toronto, ON M5G 1L7, Canada
[7]Princess Margaret Cancer Centre, University Health Network, Toronto, ON M5G 2C4, Canada
[8]Multiple Sclerosis Center of Excellence, Oklahoma Medical Research Foundation, Oklahoma City, OK 73104, USA
[9]Buck Institute for Research on Aging, Novato, CA 94945, USA
[10]Women's College Research Institute, Women's College Hospital, Toronto, ON M5G 1N8, Canada
[11]Sunnybrook Research Institute, Sunnybrook Hospital, Toronto, ON M4M 3M5, Canada
[12]Division of Cellular and Molecular Biology, Diabetes Research Group, Toronto General Hospital Research Institute, University Health Network, Toronto, ON M5G 1L7, Canada
[13]Department of Laboratory Medicine and Pathobiology, University of Toronto, ON M5S 1A8, Canada
[14]These authors contributed equally
[15]Present address: Bristol Myers Squibb, Cambridge, MA 02141, USA
[16]Lead contact
*Correspondence: bob-axtell@omrf.org (R.C.A.), shannon.dunn@utoronto.ca (S.E.D.)
https://doi.org/10.1016/j.cmet.2024.07.017

SUMMARY

Obesity has been implicated in the rise of autoimmunity in women. We report that obesity induces a serum protein signature that is associated with T helper 1 (Th1), interleukin (IL)-17, and multiple sclerosis (MS) signaling pathways selectively in human females. Females, but not male mice, subjected to diet-induced overweightness/obesity (DIO) exhibited upregulated Th1/IL-17 inflammation in the central nervous system during experimental autoimmune encephalomyelitis, a model of MS. This was associated with worsened disability and a heightened expansion of myelin-specific Th1 cells in the peripheral lymphoid organs. Moreover, at steady state, DIO increased serum levels of interferon (IFN)-α and potentiated STAT1 expression and IFN-γ production by naive $CD4^+$ T cells uniquely in female mice. This T cell phenotype was driven by increased adiposity and was prevented by the removal of ovaries or knockdown of the type I IFN receptor in T cells. Our findings offer a mechanistic explanation of how obesity enhances autoimmunity.

INTRODUCTION

Multiple sclerosis (MS) is an autoimmune disorder that targets the central nervous system (CNS) white matter.[1] This disease is thought to be initiated when autoreactive $CD4^+$ T cells become activated, differentiate into pro-inflammatory T helper 1 (Th1) and Th17 cells, and infiltrate the CNS to initiate inflammatory demyelination.[2] In support of this theory, $CD4^+$ and $CD8^+$ T cells secreting interferon (IFN)-γ, interleukin (IL)-17A, and granulocyte-macrophage colony-stimulating factor (GM-CSF) are detected in acute MS lesions,[3] and therapies that inhibit leukocyte migration into the CNS prevent MS attacks.[4] Experimental autoimmune encephalomyelitis (EAE) is a Th1/Th17 cell-mediated autoimmune disease that is induced in rodents by immunization with myelin antigens in complete Freund's adjuvant (CFA) that recapitulates many of the early pathogenic features of MS.[5,6] Although Th17 cells have been shown to have an advantage over Th1 cells in accessing the CNS compartment in EAE,[7] once on site, both Th1 and Th17 cells produce IFN-γ and GM-CSF, which license the CNS-infiltrating monocytes to produce pro-inflammatory mediators that mediate oligodendrocyte death.[6,8]

While the immunopathogenesis of EAE is well understood, how autoreactive $CD4^+$ T cells become activated in MS remains

This is an open access article under the CC BY-NC-ND license (http://creativecommons.org/licenses/by-nc-nd/4.0/).

Please cite this article in press as: Cordeiro et al., Obesity intensifies sex-specific interferon signaling to selectively worsen central nervous system autoimmunity in females, Cell Metabolism (2024), https://doi.org/10.1016/j.cmet.2024.07.017

unknown. Clues to these mechanisms have been provided by studies of the genetic polymorphisms and environmental factors that confer MS risk.[9] Carriers of the major histocompatibility complex (MHC) class II MS risk allele *HLA-DRB1*1501* have an ~3-fold higher risk of MS.[9] There is also a female preponderance of MS that manifests post-puberty, implicating female gonadal hormones in promoting autoimmunity.[10] Furthermore, the incidence of MS in females has increased over the past 5 decades, implicating changing environmental factors in disease risk.[11,12] One factor that has increased over this period, which associates with MS, is the development of obesity.[13] The association between obesity and MS is particularly strong in females who also carry the MS-related HLA risk genotype (odds ratio > 15),[14] suggesting an interaction of obesity and female sex in the promotion of Th autoimmunity in MS. The underlying mechanisms of this association remain unclear.

Here, we investigated the effect of obesity on serum proteomic signatures in men and women affected or not affected by MS and found a unique elevation of pro-inflammatory pathways including Th1, IL-17, and MS signaling pathways in females, irrespective of MS diagnosis. We then induced diet-induced obesity (DIO) in male and female mice and discovered that this treatment increased the expansion and CNS accumulation of pro-inflammatory myelin-reactive Th1 cells, especially in the females during EAE. Further studies in mice demonstrated that DIO enhanced serum IFN-α levels only in females at steady state, which associated with heightened expression of activation markers and potentiated STAT1 expression and IFN-γ production by naive $CD4^+$ T cells. Our findings offer a mechanistic explanation for the predominantly female-driven impact of obesity in enhancing autoimmunity.

RESULTS

Obesity alters pro-inflammatory proteomic signatures differently in men and women

To gain insights into how obesity alters inflammatory processes in men and women, we conducted a multiplexed proteomic analysis on the serum of females and males with relapsing-remitting MS (RRMS) and sex-matched controls not affected by MS, who were obese (body mass index [BMI] $\geq$ 30 kg/m^2) or non-obese (BMI < 30 kg/m^2) (Figures 1A–1D; see Table S1 for participant characteristics). Two thresholds of significance were applied: one more stringent (false discovery rate [FDR] = 0.1) and one less stringent (p = 0.05). Notably, 450 proteins were detected at a greater level in females with RRMS who were obese versus non-obese at $p \leq 0.05$ (368 at FDR $\leq$ 0.1) (Figure 1A; Table S2). Comparatively fewer proteins (51 at $p \leq 0.05$) were upregulated with obesity in males with RRMS (Figure 1B; Table S2). A similar sex-dependent pattern in protein changes was seen with obesity in those not affected by MS, with females showing a greater number of proteins upregulated with obesity, compared with males (245 proteins in females, 54 in males, $p \leq 0.05$) (Figures 1C and 1D; Table S2). Few proteins were downregulated with obesity in male or female MS or control participant groups (Figures 1A–1D; Table S2).

Next, the similarities and differences between the obesity-induced proteins were examined in relation to sex and disease status (Figure 1E). Surprisingly, the majority of proteins that increased with obesity were distinct between men and women (Figure 1E; Table S2). Only one protein, the adipokine leptin, was increased in all four groups (Figure 1E; Table S2). By contrast, 146 proteins were commonly upregulated with obesity in control and RRMS female groups (Figure 1E; Table S2).

Ingenuity pathway analysis (IPA) of the differently abundant proteins was performed, and this detected several inflammatory pathways that were increased solely in females with obesity (Figure 1F; Table S3). These included S100, cytokine storm, Th1, IL-17, IL-6, dendritic cell maturation, and MS signaling pathways. The activation of IRF pathway was also upregulated with obesity in the females with RRMS (Figure 1F; Table S3). The heatmap in Figure 1G and data in Table S2 illustrate how sex, obesity, and disease status affected the crosstalk among proteins in some of the top upregulated pathways. When considering key proteins in these pathways, leptin and IL-6 (in the IL-17 pathway) showed evidence of a dose-dependent upregulation with increasing BMI in both males and females (Figures S1A and S1B), whereas IL-12p70 (in the Th1 pathway) and the RNA sensor RIG-I (in the IRF pathway) were significantly elevated with increasing BMI only in females with RRMS (Figures S1C and S1D), indicating a potential sex-disease interaction in the effect of obesity on expression of these proteins.

Because there was an incomplete overlap in the proteins that mapped to significant pathways in female MS and control groups (Table S2), and given the overrepresentation of individuals who self-identified as White in the MS cohort (Table S1), we conducted further analyses specifically focusing on participants who self-identified as White. We found that most of the proteins upregulated with obesity in the whole cohort of MS or control participants were still significant at p = 0.05 (uncorrected) in the Whites-focused analyses (Table S2). Furthermore, IPA identified the same pathways to be increased with obesity in White control and MS females (Figure S1E; Table S3). In sum, inflammatory signatures vary markedly between the sexes with obesity.

DIO enhances EAE severity more in female mice

To gain insights into the biological mechanisms underpinning the sex-dependent increase in Th1 and IL-17 pathways with obesity and to evaluate the impact of this biology on autoimmunity, we modeled a DIO state in adolescent (6-week-old) male and female C57BL/6J mice by high-fat diet (HFD) feeding; controls were fed normal chow diet (NCD). Preliminary studies established that it took 4 weeks of HFD feeding for both male and female mice to show significant body weight increases over NCD-fed controls (Figure S2A). At this time, both males and females showed greater fat pad weights but had not yet developed hyperglycemia or insulin resistance (Figures S2B–S2E). While male C57BL/6J mice were glucose intolerant at 4 weeks of HFD feeding, females remained glucose sensitive (Figures S2F and S2G). Given the requirement of 4 weeks of HFD feeding to achieve fat gains in females, this duration of diet treatment was used for subsequent studies.

Next, we investigated the effect of DIO on the development of CNS autoimmunity. Male and female mice were placed on HFD (DIO) or NCD (CTRL) for 4 weeks, and then EAE was induced by immunization with myelin oligodendrocyte glycoprotein peptide 35–55 ($MOG_{35–55}$)/CFA and pertussis toxin (PTX) injections. We observed that DIO increased the severity of EAE in both sexes, but this effect was more prominent in the females (Figures 2A

Please cite this article in press as: Cordeiro et al., Obesity intensifies sex-specific interferon signaling to selectively worsen central nervous system autoimmunity in females, Cell Metabolism (2024), https://doi.org/10.1016/j.cmet.2024.07.017

CellPress
OPEN ACCESS

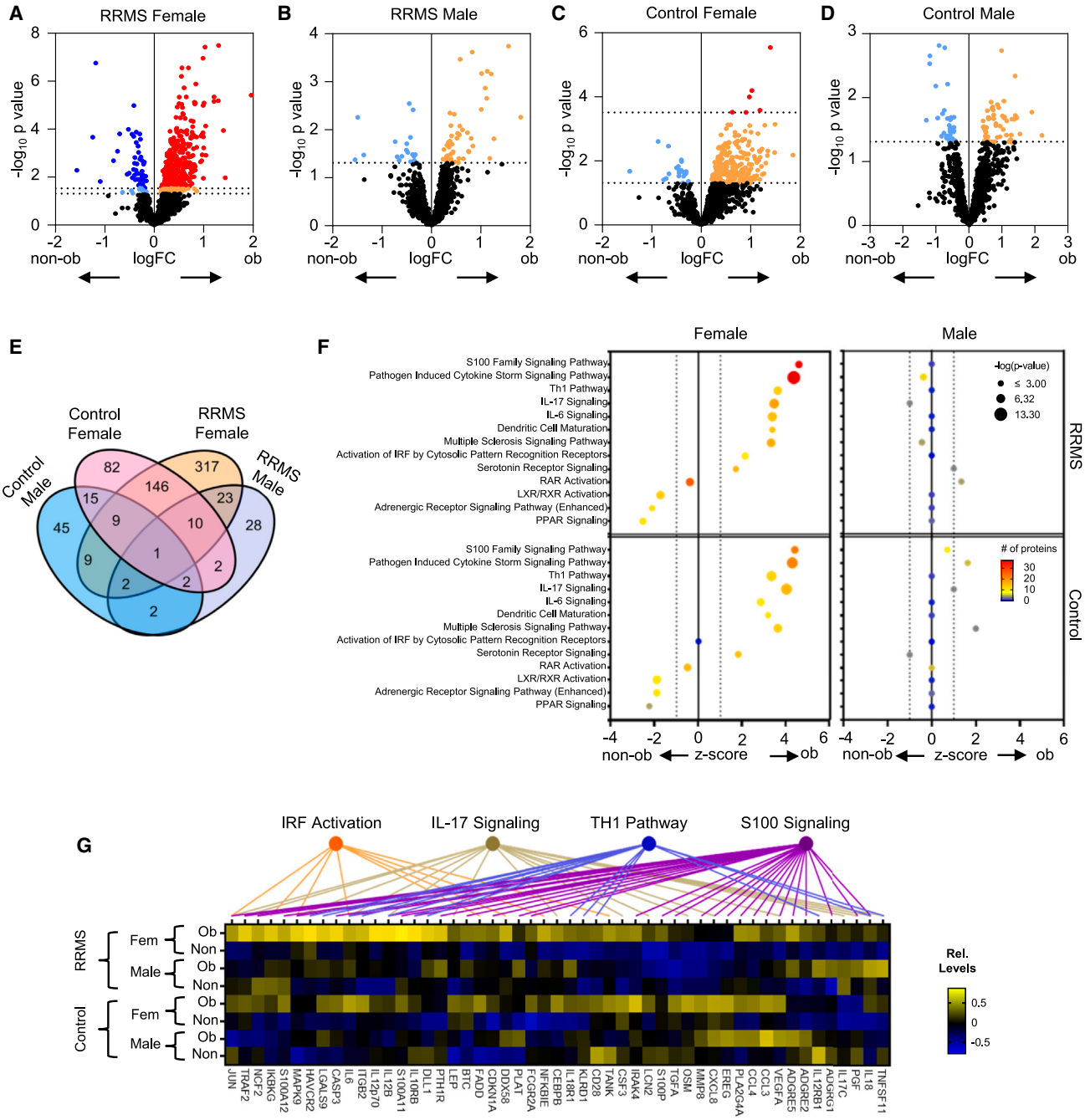

Figure 1. Obesity uniquely elevates Th1 and IL-17 inflammatory pathways in female humans

(A–D) Comparison of serum protein profiles of obese and non-obese male and female individuals with or without RRMS. Red and dark blue, respectively, denote proteins elevated or reduced by obesity at FDR = 0.1. Orange and light blue, respectively, denote proteins elevated or reduced by obesity at $p \leq 0.05$. Analyses were adjusted for age and ethnicity.

(E) Venn diagram showing the number of proteins increased with obesity between each comparison ($p \leq 0.05$).

(F) Ingenuity pathway analysis (IPA) of signaling pathways altered in obesity. Shown are the Z scores (x axis), $-\log_{10} p$ values (size indicated by symbol size), and number of proteins in each pathway (heatmap legend) as determined using IPA.

(G) Heatmap depicting differentially abundant serum proteins that mapped to IRF activation, IL-17 signaling, Th1, and S100 signal pathways.

See also Figure S1 and Table S2.

and 2B). Although DIO and control mice exhibited a similar timing of EAE onset (Figure 2C), peak and cumulative scores were greater than those of controls only in the female DIO group (Figures 2D and 2E). Histological analysis of the spinal cords at endpoint also revealed greater demyelination in the DIO relative to the control females (Figures 2F–2J).

Please cite this article in press as: Cordeiro et al., Obesity intensifies sex-specific interferon signaling to selectively worsen central nervous system autoimmunity in females, Cell Metabolism (2024), https://doi.org/10.1016/j.cmet.2024.07.017

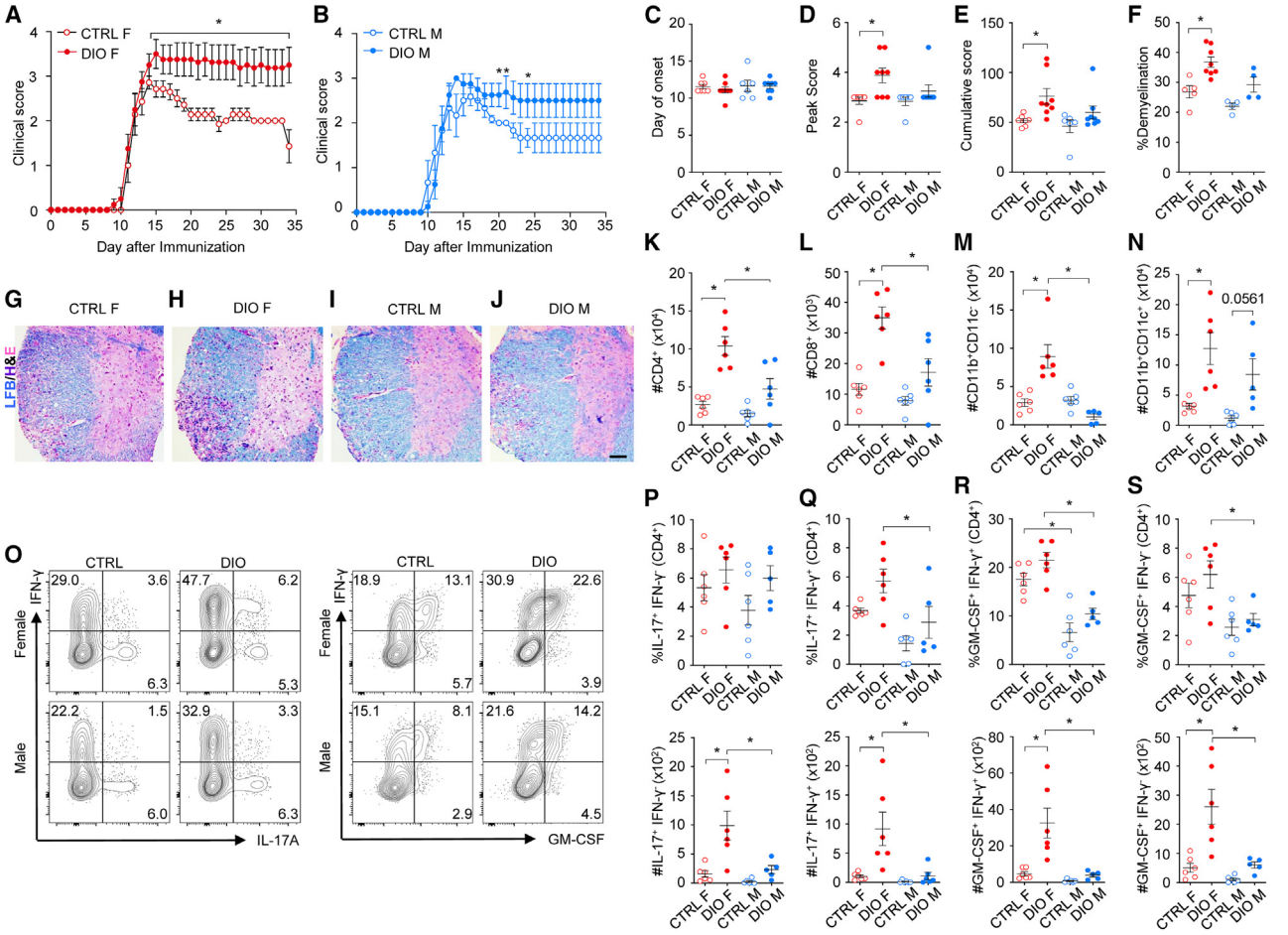

Figure 2. Diet-induced obesity increases EAE severity, especially in female mice

EAE was induced in control and DIO C57BL/6J mice with $MOG_{35–55}$/CFA and PTX.

(A and B) Clinical scores of female (A) and male (B) mice.

(C) Day of symptom onset.

(D) Peak clinical score.

(E) Cumulative disease score.

(F) Percentage of demyelinated white matter in thoracic spinal cord.

(G–J) Representative images of H&E- and luxol fast blue (LFB)-stained thoracic spinal cord sections. Scale bars, 50 μm.

(K–N) Total numbers of $CD4^+$ T cells (K), $CD8^+$ T cells (L), $CD45^{hi}CD11b^+CD11c^-$ cells (M), and $CD45^{hi}CD11b^+CD11c^+$ cells (N) in the CNS at 2–4 days post-symptom onset.

(O) Representative intracellular cytokine staining in the live $CD4^+$ gate after phorbol 12-myristate 13-acetate (PMA)/ionomycin restimulation.

(P–S) Frequency (top) and number (bottom) of $CD4^+$ T cells staining for the indicated cytokines.

Data are presented as mean ± SEM.

Data points in (C)–(F), (K)–(N), and (P)–(S) are individual mice from one experiment that is representative of three performed. *$p \leq 0.05$ between groups as determined by two-tailed Mann-Whitney U test (A and B) or two-way ANOVA and Bonferroni post hoc test (C–S).

We next characterized immune cell infiltration in the CNS at the onset of EAE symptoms using flow cytometry (Figure S2H). DIO female mice exhibited a significantly greater number of $CD4^+$ T cells, $CD8^+$ T cells, $CD11b^+CD11c^-$ cells, $CD11b^+CD11c^+$ cells, and microglia, but not B cells or neutrophils, compared with that in female controls (Figures 2K–2N and S2I–S2K). Intracellular cytokine staining revealed that DIO females exhibited a greater CNS accumulation of all pro-inflammatory $CD4^+$ T cell subsets examined (Figures 2O–2S), including the IFN-γ^+ IL-17^+ $CD4^+$ T cells, which are enriched in MOG-specific T cells[8] (Figures 2O and 2Q). These immune cell subsets were not increased in the males with DIO (Figures 2P–2S). The expressions of IFN-γ and GM-CSF in $CD4^+$ T cells were also greater overall in the females (Figures S2L–S2N). Thus, DIO enhanced the CNS accumulation of pro-inflammatory IFN-γ-producing $CD4^+$ T cells especially in female mice during EAE.

MOG-specific Th1 cells expand more in female mice during DIO

Since increased T cell infiltration seemed to underlie the more severe EAE phenotype in females with DIO, we evaluated $MOG_{35–55}$-specific Th responses in the peripheral lymphoid

Please cite this article in press as: Cordeiro et al., Obesity intensifies sex-specific interferon signaling to selectively worsen central nervous system autoimmunity in females, Cell Metabolism (2024), https://doi.org/10.1016/j.cmet.2024.07.017

CellPress
OPEN ACCESS

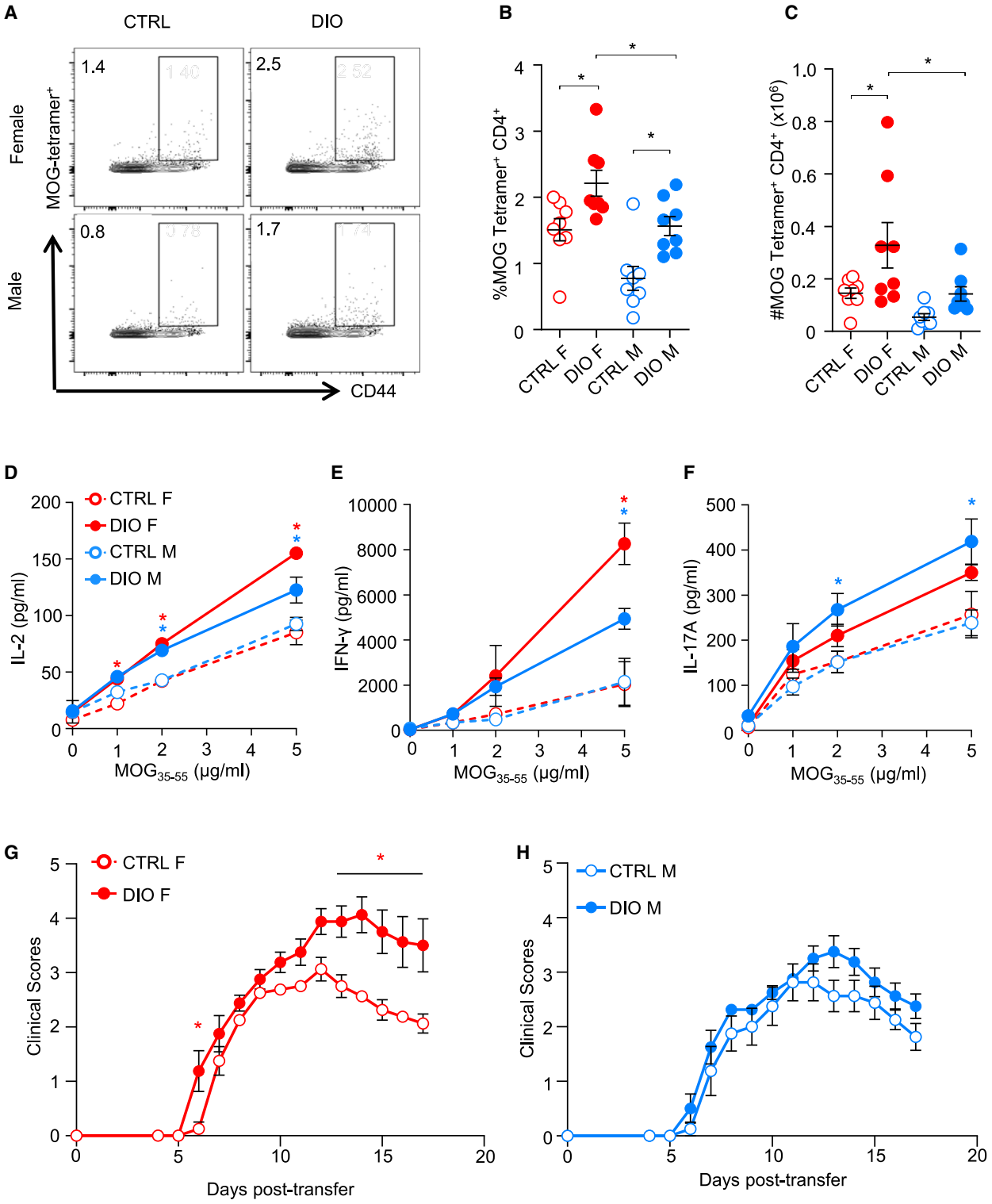

Figure 3. DIO increases Th1 responses predominantly in female mice during EAE

(A–C) Representative staining of splenic IA^b-MOG-specific tetramer$^+$ $CD44^+$ $CD4^+$ T cells in male or female $MOG_{35–55}$/CFA-injected CTRL or DIO C57BL/6J mice (A). Frequencies (B) and total numbers (C) of IA^b-MOG-specific tetramer$^+$ $CD4^+$ T cells. Data points are individual mice.

(D–F) Spleen and draining lymph node cells from mice were pooled and cultured in the presence of $MOG_{35–55}$. Supernatants were collected for ELISA measurement of IL-2 (D), IFN-γ (E), and IL-17A (F). Shown are mean ± SEM of triplicate wells from one experiment of $n = 3$ performed using pooled mice.

(legend continued on next page)

Please cite this article in press as: Cordeiro et al., Obesity intensifies sex-specific interferon signaling to selectively worsen central nervous system autoimmunity in females, Cell Metabolism (2024), https://doi.org/10.1016/j.cmet.2024.07.017

organs of control and DIO mice prior to development of EAE symptoms. We found that DIO increased the frequency of $MOG_{35–55}$-specific $CD4^+$ T cells in the spleens of male and female mice (Figures 3A and 3B); however, the number of MOG-specific $CD4^+$ T cells was increased only in the females with DIO (Figure 3C). DIO also enhanced $MOG_{35–55}$-elicited IFN-γ, IL-2, and IL-17 responses in both male and female mice; however, the extent of the increase in IFN-γ was greater in the females (Figures 3D–3F). This finding of increased Th1 and IL-17 inflammation in females with DIO mirrors the serum inflammatory signatures detected in human females with obesity.

To address whether the effect of DIO on $MOG_{35–55}$-specific T cells underpinned the more severe EAE phenotype in females, adoptive transfer EAE experiments were performed where diet was varied in the donor male or female $MOG_{35–55}$/CFA-immunized mice. At day 9 post-immunization, donor cells from the draining lymph nodes and spleens were re-activated *in vitro* in the presence of $MOG_{35–55}$ and IL-12 and were transferred into naive male C57BL/6J recipients. $MOG_{35–55}$-activated cells from the female DIO donors elicited more severe EAE, compared with those from control females (Figure 3G). Significant differences in clinical scores were not observed after transfer of control and DIO male cells (Figure 3H). These results link the peripheral Th cell phenotype to the more severe EAE seen in female mice with DIO.

Increased Th1 response in female mice with DIO is linked to increased adiposity

Next, we investigated the biological cause of the female-preponderant increase in Th1 inflammation with DIO. Since DIO affects the microbiome and since the microbiome can modify EAE,[15,16] we examined the structure and composition of the fecal microbiome in male and female mice fed NCD or HFD at steady state using 16S rRNA sequencing. Notably, 4 weeks of HFD feeding reduced the number of observed unique amplicon sequence variants (ASVs) in male and female mice, but this did not translate into significant changes in the richness of the microbiome (Figures S3A and S3B). Principal-component analysis of the weighted unique fraction metric revealed differences in beta diversity with HFD feeding (specifically, *Firmicutes* were increased and *Bacteroidota* were decreased with HFD), but mice clustered according to diet not sex (Figures S3C–S3E). Thus, sex differences in Th1 inflammation with DIO did not appear to be driven by sex-dependent changes in the microbiome.

We also conducted 4-week HFD-feeding studies in SJL/J mice, which are resistant to weight gain when fed HFD[17,18] (Figures S3H–S3J). Proteolipid protein (PLP) $peptide_{139–151}$-elicited T cell IFN-γ responses were not different between HFD- or NCD-fed SJL/J mice in spleen and draining lymph node cells following $PLP_{139–151}$/CFA immunization (Figure S3K), suggesting that weight gain was required for the increased Th1 inflammation seen with DIO.

We also employed a post-natal overnutrition (PNO) model to induce weight gain in C57BL/6J mice. In this model, litter sizes are reduced to 3 pups/dam (PNO group). Pups from small litters consume more milk and experience greater body weight gains during post-natal development than pups from larger litters (controlled at 8 pups/dam), both before and after weaning on NCD (Figures S4A–S4C)[19]; however, only female PNO mice show greater fat mass when compared to controls (Figures S4D and S4E). In contrast to DIO, PNO did not alter the microbiome composition or structure (Figures S4F–S4J). Following $MOG_{35–55}$/CFA immunization, PNO females exhibited greater $MOG_{35–55}$-elicited T cell proliferation and IFN-γ production, compared with controls, whereas IL-17 was not altered (Figures S4K–S4M). PNO females also developed a comparatively more severe course of EAE than controls (Figures S4N and S4O). These results suggest that the enhanced Th1 immunity with DIO was due to increased adiposity.

Increased Th1 inflammation induced in female mice with DIO is T cell intrinsic and is promoted by ovarian hormones, but not leptin

We were intrigued that DIO promoted myelin-specific Th1 cell immunity only in the females, despite males showing greater fat gains. Thus, we conducted studies to determine the cellular basis of the sex-dependent increase in Th1 inflammation with DIO. We first evaluated the $CD4^+$ T cell compartment in NCD- and HFD-fed male and female mice. While the number of $CD4^+$ T cells did not differ between DIO and control mice of either sex at steady state (Figure 4A), the percentages of $CD4^+$ T cells that were $FoxP3^+CD25^+$, $CD25^+$, or $CD44^{hi}$ and CD44 expression were elevated uniquely in the females with DIO (Figures 4B–4E). We also evaluated the *in vitro* functionality of Treg isolated from the different groups and found that $CD4^+CD25^{hi}$ Treg from DIO male or female mice did not exhibit a differential capacity to suppress the proliferation of sex-matched $CD4^+CD25^-$ cells (Figures 4F and 4G). In addition, splenic $CD11c^+$ dendritic cells isolated from control or DIO male or female mice exhibited an equivalent ability to prime $MOG_{35–55}$-reactive $CD4^+$ T cell receptor (TCR) transgenic cells *in vitro* (Figures 4H and 4I).

We next sorted naive ($CD44^{lo}$) $CD4^+$ T cells from male and female DIO and control mice and evaluated the ability of these cells to proliferate and secrete cytokines in response to stimulation with anti-CD3 and anti-CD28. These studies revealed that naive $CD4^+$ T cells from DIO female mice proliferated equivalently and produced similar levels of IL-2 (Figures 4J and 4K), but they produced markedly higher levels of IFN-γ, compared with NCD female cells (Figure 4L). Although a small effect of DIO in increasing $CD4^+$ T cell IFN-γ production was seen in the males, it was much less pronounced than in females (Figure 4L). Taken together with the *in vivo* studies, these findings suggest that DIO may enhance Th1 inflammatory mechanisms in EAE by increasing (1) T cell activation, (2) myelin-specific Th cell expansion, and (3) the potential of the $CD4^+$ T cells to produce IFN-γ.

Th1 polarization of naive $CD4^+$ T cells is associated with two waves of expression of the Th1 lineage-determining factor

(G and H) Spleen and draining lymph node cells were collected, pooled, and cultured with $MOG_{35–55}$ and IL-12p70 for 3 days and adoptively transferred into naive recipient male C57BL/6J mice. Mean ± SEM daily clinical scores after transfer of cells from female (G) or male (H) mice. n = 7–8 per group.
*$p \leq 0.05$ significance determined using a two-way ANOVA and Bonferroni post hoc test (B–F) or two-tailed Mann-Whitney U test (G and H). In (D)–(H), blue and red asterisks indicate differences between CTRL and DIO males and between CTRL and DIO females, respectively.

Please cite this article in press as: Cordeiro et al., Obesity intensifies sex-specific interferon signaling to selectively worsen central nervous system autoimmunity in females, Cell Metabolism (2024), https://doi.org/10.1016/j.cmet.2024.07.017

CellPress
OPEN ACCESS

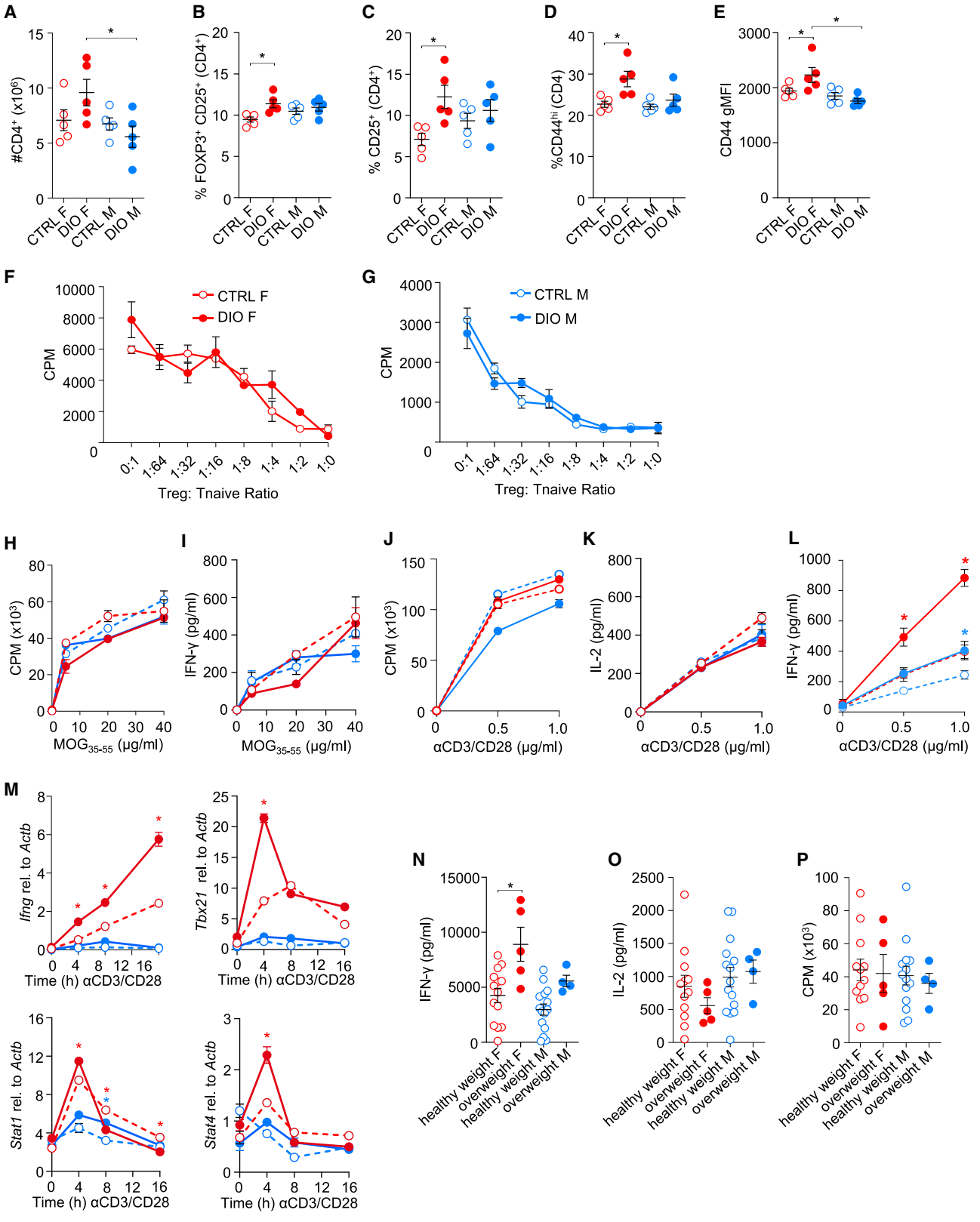

(legend on next page)

Please cite this article in press as: Cordeiro et al., Obesity intensifies sex-specific interferon signaling to selectively worsen central nervous system autoimmunity in females, Cell Metabolism (2024), https://doi.org/10.1016/j.cmet.2024.07.017

T-bet.[20] The first (≤48 h) is driven by autocrine IFN-γ/IFN-γ receptor (IFN-γR)/STAT1 signaling and serves to induce T-bet and IL-12 receptor β2 expression.[20,21] The second is driven by IL-12 and is crucial for Th1 lineage stabilization.[20] To address whether early events in Th1 differentiation are enhanced by DIO, we measured the expressions of *Ifng* and other key genes involved in Th1 programming in male and female control and DIO naive CD4$^+$ T cells after anti-CD3/anti-CD28 stimulation. DIO potentiated the expressions of *Ifng*, *Tbx21*, *Stat1*, and *Stat4* in female CD4$^+$ T cells even at early time points of stimulation (Figure 4M), suggesting that the activity of the TCR/IFN-γR/STAT1 signaling loop may be enhanced in female naive CD4$^+$ T cells with DIO. Female CD4$^+$ T cells also exhibited an overall greater expression of these Th1-related genes, compared with male CD4$^+$ T cells (Figure 4M).

To explore whether greater BMI is associated with potentiated T cell IFN-γ production in humans, a study was done where peripheral blood naive (CD45RA$^+$) CD4$^+$ T cells were isolated from male and female donors having an overweight (25.0–29.9 kg/m^2) or healthy weight (20.0–24.9 kg/m^2) BMI. These cells were stimulated *in vitro* with anti-CD3/anti-CD28. Similar to our findings in mice, CD45RA$^+$ CD4$^+$ T cells from overweight females produced greater levels of IFN-γ than those from healthy weight females; there was no significant difference in IFN-γ production between healthy weight and overweight male T cells (Figure 4N). Furthermore, no effect of BMI or sex on the proliferation of CD4$^+$ T cells or IL-2 production was observed (Figures 4O and 4P).

We also investigated whether the DIO-induced Th cell phenotype in female mice is reversible. For this experiment, C57BL/6J female mice were provided (1) NCD for 4 weeks and then placed on HFD for 4 weeks, (2) HFD for 4 weeks and then switched to NCD for 4 weeks (DIET mice), or (3) NCD throughout. Female DIET mice exhibited similar body and fat pad weights at endpoint as female mice maintained on NCD (Figures S4P–S4R). DIET mice also exhibited an immune profile that was more similar to control than DIO mice with comparable percentages of CD44^{hi} CD4$^+$ T cells, CD44 expression, and splenic T cell production of IFN-γ in response to anti-CD3/anti-CD28 stimulation (Figures S4S–S4U). Thus, the T cell phenotype changes seen in the female mice with short-term DIO are reversible with weight loss.

The effect of female sex in potentiating the DIO effect on T cell IFN-γ production suggested that female gonadal hormones may be promoting this T cell phenotype. We therefore repeated *in vitro* Th cell stimulation assays with naive CD4$^+$ T cells from HFD or NCD female mice that had received sham or pre-pubertal ovariectomy (OVX) surgery at 4 weeks of age. Consistent with past reports,[22] OVX mice exhibited greater weight gains than sham-operated controls when fed HFD (Figures 5A–5C); despite this, the effect of DIO in increasing IFN-γ by activated naive CD4$^+$ T cells was severely blunted (Figure 5D). The proliferation of the naive CD4$^+$ T cells was unperturbed by either DIO or OVX treatment (Figure 5E). These findings suggest that ovarian hormones are permissive for the effect of DIO in increasing CD4$^+$ T cell IFN-γ production.

It has been speculated that the effect of obesity on MS is due to increased pro-inflammatory adipokine production.[23] We therefore profiled adipokines and cytokines in the serum of control and DIO male and female mice. Of the adipokines detected, IL-6 and leptin were significantly increased, and tumor necrosis factor (TNF) tended to be increased with DIO (Figures S5A–S5C). Adiponectin, which can be inflammatory in MS,[24] was reduced, whereas the levels of PAI-1 and resistin were not altered with DIO (Figures S5D–S5F).

Since past studies have reported an effect of leptin in promoting IFN-γ production by MS patient T cells[25] and myelin-reactive T cells in EAE,[26] we investigated the involvement of leptin signaling in the heightened T cell IFN-γ production with DIO. To this end, we generated female mice that had leptin-receptor deficiency restricted to CD4$^+$ T cells (LepR CD4$^+$ T-KO) using a mixed bone marrow chimera (BMC) approach (Figures S5G and S5H). These mice and female controls were fed HFD or NCD starting at 8 weeks post-BM transfer. LepR CD4$^+$ T-KO mice gained a similar amount of weight on HFD as wild-type (WT) BMC mice (Figure S5I); however, CD4$^+$ T cells from these mice did not exhibit diminished T cell IFN-γ production with DIO (Figure S5J). Comparable findings were observed in experiments that used LepR floxed mice where deletion in T cells was driven by the Lck-Cre distal transgene (Figures S5K–S5N). Thus, DIO did not appear to be enhancing T cell IFN-γ production through increased leptin signaling.

DIO enhances ISG expression and IFN-γR/STAT1 signaling in female CD4$^+$ T cells

To gain insights into the molecular basis of the increased IFN-γ production by female CD4$^+$ T cells with DIO, we compared the

Figure 4. Increased Th1 responses in females with DIO are driven by T cell-intrinsic differences

(A–M) Male and female C57BL/6J mice were treated to NCD (CTRL) or HFD (DIO) for 4 weeks.

(A) Number of splenic CD4$^+$ T cells.

(B–D) Frequency of splenic CD4$^+$ T cells that were FoxP3$^+$CD25$^+$ (B), CD25$^+$ (C), or CD44^{hi} (D).

(E) Geometric mean fluorescent intensity (gMFI) of CD44 on CD4$^+$ T cells.

(F and G) CD4$^+$CD25^{hi} (Treg) and CD4$^+$CD44$^{low\text{-}int}$CD25$^-$ (Tnaive) cells from female (F) and male (G) mice were co-cultured at the indicated ratios with sex-matched Tnaive cells, irradiated splenocytes, and soluble anti-CD3. Proliferation of T cells was measured by [^{3}H]-thymidine incorporation assay in counts per minute (CPM).

(H and I) Splenic CD11c$^+$ DCs from CTRL and DIO mice were co-cultured with sex-matched MOG$_{35–55}$-specific 2D2 CD4$^+$ T cells with 0–40 μg/mL MOG$_{35–55}$. (H) Proliferation in CPM was measured by [^{3}H]-thymidine incorporation assay. (I) IFN-γ in supernatants.

(J–L) Naive CD4$^+$ T cells were sorted from NCD or DIO mice and were cultured with increasing amounts of anti-CD3/anti-CD28. (J) Proliferation was measured by [^{3}H]-thymidine incorporation assay. IL-2 (K) and IFN-γ (L) in supernatants.

(M) Relative mRNA expressions of *Ifng*, *Tbx21*, *Stat1*, and *Stat4* in naive CD4$^+$ T cells stimulated with anti-CD3/anti-CD28 after normalization to β-actin.

(N–P) PBMCs were collected from human participants with healthy weight (20.0–24.9 kg/m^2) or overweight (25.0–29.9 kg/m^2) BMIs. Naive CD45RA$^+$ CD4$^+$ T cells were stimulated *in vitro* with anti-CD3/anti-CD28-coated Dynabeads. IFN-γ (N) and IL-2 (O) were measured in supernatants by ELISA. (P) Proliferation (CPM) was measured by [H^3]-thymidine incorporation assay. Data points are individual people.

Values are means ± SEM. Data in mice are representative of 2–5 independent experiments. Significant differences were determined by two-way ANOVA with Bonferroni post hoc test (A–E and H–P) or by Mann-Whitney two-tailed t test (F and G). *$p \leq 0.05$.

Please cite this article in press as: Cordeiro et al., Obesity intensifies sex-specific interferon signaling to selectively worsen central nervous system autoimmunity in females, Cell Metabolism (2024), https://doi.org/10.1016/j.cmet.2024.07.017

CellPress
OPEN ACCESS

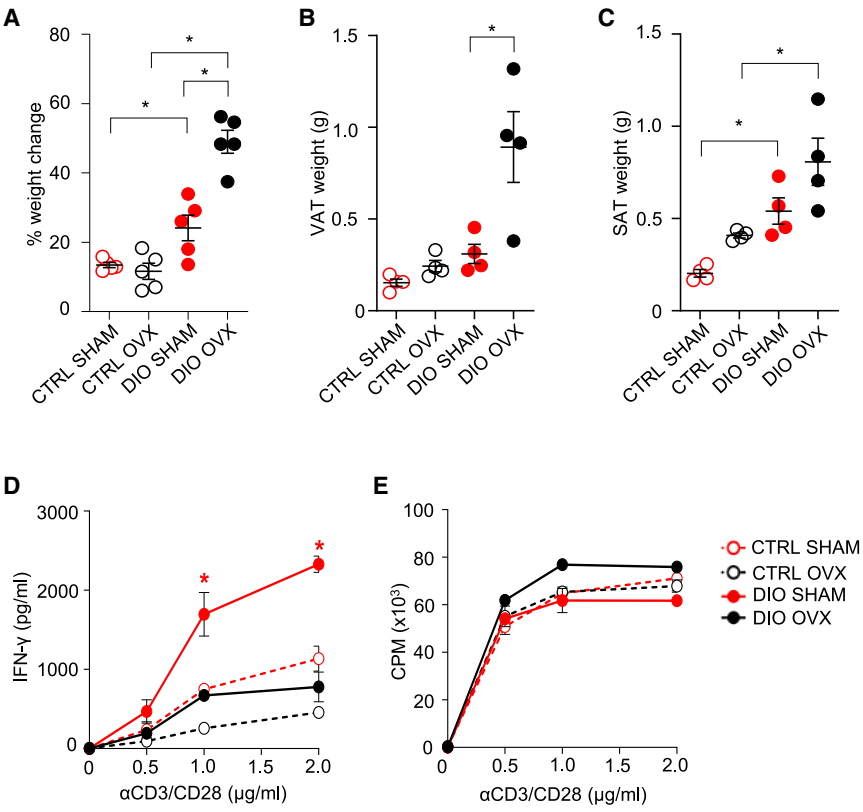

Figure 5. Ovarian hormones accentuate Th1 cytokine production by female T cells with DIO

Four-week-old female C57BL/6J mice underwent pre-pubertal ovariectomy (OVX) or sham surgery (sham). At 6 weeks of age, mice were placed on HFD or NCD for 4 weeks, prior to data collection at 10 weeks of age.

(A) % body weight change over 4 weeks of the diets.

(B and C) Endpoint visceral adipose tissue (VAT) (B) and subcutaneous adipose tissue (SAT) (C) weight.

(D and E) Naive $CD44^{lo\text{-}int}$ $CD4^+$ cells were isolated from mice (n = 5/group) and were cultured in the presence of anti-CD3/anti-CD28. Cytokines in supernatants (D) and proliferation (CPM) (E) by [^{3}H]-thymidine incorporation assay.

Data points represent individual mice (A–C) or mean ± SEM of triplicate wells of pooled mice (D and E) in one experiment that was representative of two performed. Differences determined by two-way ANOVA and Bonferroni post hoc test. *$p \leq 0.05$.

transcriptomic profiles of naive $CD4^+$ T cells that were isolated from control and DIO female mice. RNA was isolated from quiescent cells or at 16 h after *in vitro* stimulation with anti-CD3/anti-CD28. Quiescent naive $CD4^+$ T cells exhibited an upregulation of 86 unique transcripts with DIO (fold cutoff > 1.2; Table S4). Gene Ontology (GO) analysis revealed upregulation of small nuclear RNAs, genes related to T cell adhesion/migration (*Vcam*, *Rhob*, *Adgre4*, *Itga3*, *Itgb5*, and *Cxcr4*), the misfolded protein response (*Dnajb1*, *Hspa8*, and *Hsph1*), cytosolic RNA sensing (*Ddx58*), and lipid uptake and metabolism (*Lrp1*, *Plin2*, *Abca1*, *Pltp*, *Cpt1a*, and *Slc25a20*).

A comparatively greater number of transcripts were upregulated in activated female $CD4^+$ T cells with DIO (Table S4). Top upregulated pathways were related to "response to IFN-γ" (Figure 6A; Table S5). Comparison of upregulated genes against published lists of Th lineage genes[27] confirmed the presence of a strong Th1 gene signature in DIO female $CD4^+$ T cells (Figure 6B; Table S5); these Th1-associated genes included *Stat1*, which signals downstream of IFN-γR, and *Il7r* and *Il18r1*, which are involved in terminal Th1 differentiation[28–30] (Figure 6B). DIO $CD4^+$ T cells also expressed higher levels of *Il6ra* and *Il17a*, thereby explaining their proneness for IL-17A secretion (Figure 6B). Very few transcripts were downregulated in $CD4^+$ T cells with DIO (Table S6).

The heightened IFN signature seen in the female DIO $CD4^+$ T cells led us to compare the list of differentially expressed transcripts against the IMMGEN dataset of type I IFN- and type II IFN-regulated genes in murine $CD4^+$ T cells.[31] This analysis revealed that ~50% of upregulated transcripts with DIO were IFN-stimulated genes (ISGs) (Figure 6C; Tables S7 and S8). In the quiescent naive $CD4^+$ T cells, a greater number of type I ISGs were detected, whereas stimulated $CD4^+$ T cells exhibited a stronger type II ISG signature.

Since STAT1, IL-18 receptor, and IL-7 receptor signaling are directly situated in the Th1 signaling pathway, we validated the expressions of these proteins in naive $CD4^+$ T cells from control and DIO female mice by flow cytometry. This analysis confirmed that female naive $CD4^+$ T cells from DIO mice expressed greater levels of STAT1 and IL-18Rα, but not IL-7Rα (Figures 6D–6F). STAT1 and IL-18Rα were not increased in male naive $CD4^+$ T cells with DIO (Figures S6A and S6B), indicating that these proteins were upregulated in a sex-specific manner with DIO.

To investigate the activity of the IFN-γR/STAT1 signaling loop in early Th1 differentiation, the phosphorylation of STAT1 (Y701) (pSTAT1) in naive $CD4^+$ T cells of DIO and control female mice was measured after *in vitro* stimulation with IFN-γ (Figure 6G). Naive female $CD4^+$ T cells from DIO mice had greater peak pSTAT1 post-IFN-γ stimulation, compared with controls (Figure 6G). We also detected a positive correlation between the % body weight change over 4 weeks with the diets and the peak geometric mean fluorescent intensity (gMFI) of pSTAT1 in naive $CD4^+$ T cells of individual female mice (Figure 6H).

DIO induces type I IFN that promotes T cell STAT1 and IFN-γ expression and drives more severe EAE in females

STAT1 is engaged downstream of type I and II IFN receptors. Since IFN-γ was not elevated in the serum of female mice with DIO (Figure 6I), we focused our attention on type I IFNs, which had not been captured by our multiplex cytokine assay. We found that the levels of IFN-α, but not IFN-β, were increased in the sera of female mice with DIO; this increase in IFN-α was not seen in the males (Figures 6J and 6K). The levels of IFN-α

Please cite this article in press as: Cordeiro et al., Obesity intensifies sex-specific interferon signaling to selectively worsen central nervous system autoimmunity in females, Cell Metabolism (2024), https://doi.org/10.1016/j.cmet.2024.07.017

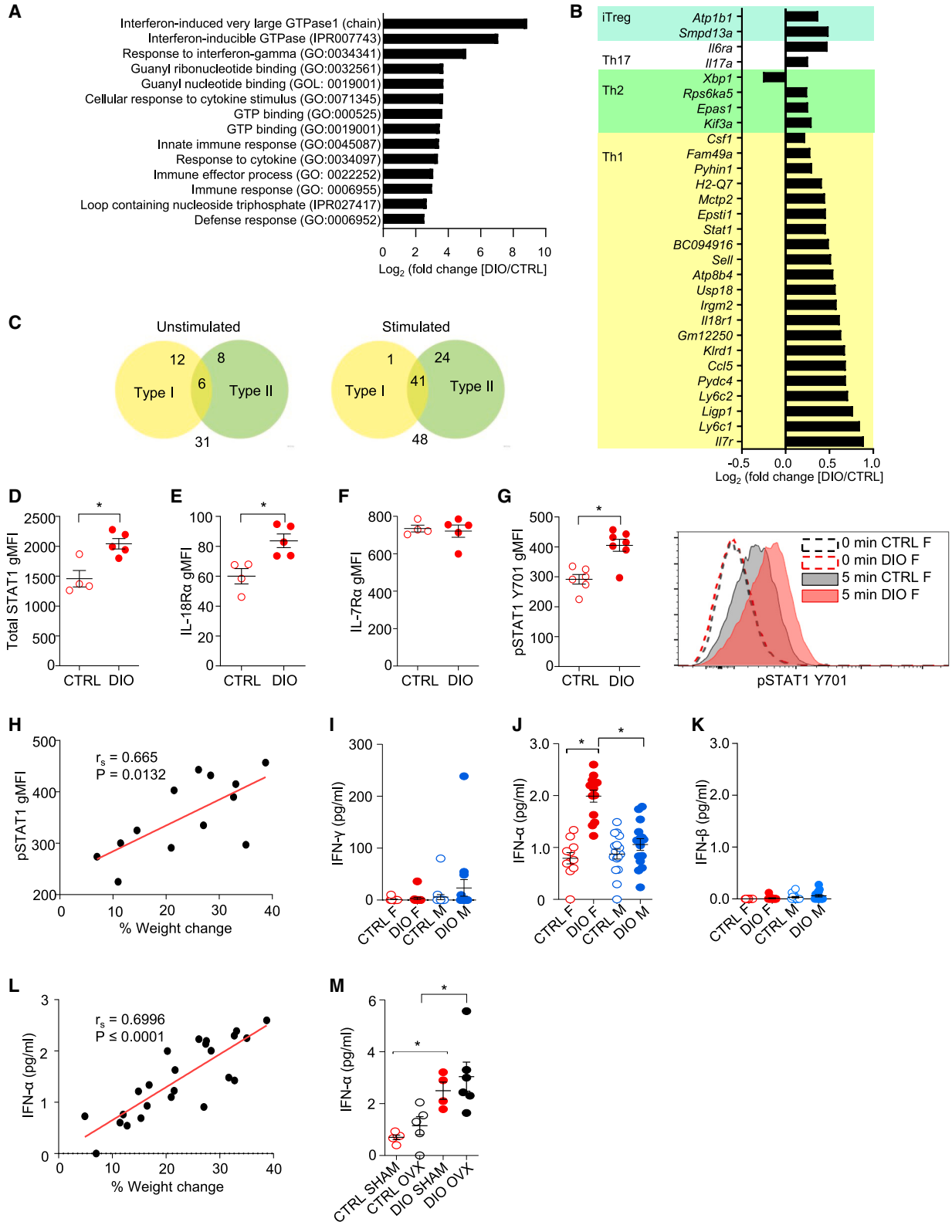

(legend on next page)

Please cite this article in press as: Cordeiro et al., Obesity intensifies sex-specific interferon signaling to selectively worsen central nervous system autoimmunity in females, Cell Metabolism (2024), https://doi.org/10.1016/j.cmet.2024.07.017

CellPress
OPEN ACCESS

in the serum of individual DIO and control female mice also correlated with % body weight gain with the diets (Figure 6L). To address whether ovarian hormones promoted Th1 cytokine production through increases in IFN-α, we also measured IFN-α levels in the serum of OVX- and sham-operated female mice fed HFD and NCD; however, this analysis revealed that sham and OVX females exhibited a similar rise in IFN-α levels with DIO (Figure 6M). Together, these findings suggested that increased IFN-α signaling may be driving the ISG signature in female CD4$^+$ T cells with DIO and that ovarian hormones potentiated T cell IFN-γ production downstream of IFN-α production.

To specifically address the involvement of IFN-α signaling in the DIO-induced T cell phenotype in female mice, we generated mice that were deficient in type I receptor alpha chain (IFNAR1) selectively in T cells by crossing IFNAR1 floxed mice with mice that expressed Cre recombinase under the control of the distal Lck-Cre promoter (IFNAR T-KO): IFNAR T-KO mice were compared with littermate controls that were homozygous for the IFNAR floxed allele and negative for the Cre allele (flox) (Figures 7A and S6C–S6G). Both IFNAR T-KO and flox female mice gained an equivalent amount of body weight and fat mass with HFD (Figures 7B–7D). Examination of CD4$^+$ T cells in the peripheral immune compartment revealed the expected increase in the expressions of CD44, IL-18Rα, and STAT1 and IFN-γ secretion by female flox CD4$^+$ T cells with DIO (Figures 7E–7H). All these measures were attenuated in the DIO IFNAR T-KO mice, with STAT1 expression and IFN-γ secretion being even lower than seen in the flox CTRL group (Figures 7E–7H). These findings suggest that type I IFN signaling mediates the effect of DIO on these T cell measures but also maintains the basal expression of STAT1 and IFN-γ in CD4$^+$ T cells.

We then investigated whether IFNAR T-KO mice would be protected from the effects of DIO on EAE. As anticipated, DIO enhanced the severity of EAE in female CTRL flox mice, but this effect was not seen in the female IFNAR T-KO mice (Figures 7I–7K), which instead showed a delay in disease onset (Figure 7L). No significant effect of DIO or genotype on EAE was observed in the males (Figures S6H–S6K). In addition, upon evaluating myelin-specific Th cell responses during EAE, we observed that female IFNAR T-KO mice exhibited a reduced percentage of Th1 effector cells (IFN-γ$^+$CD44^{hi} CD4$^+$ T cells) (Figures 7M and 7N) and decreased myelin-specific Th1 responses (Figure S6L) in the peripheral lymphoid organs, as compared with flox CTRL mice. Interestingly, the percentages of IL-17$^+$ CD4$^+$ T cells, which increased with DIO, were not impacted by IFNAR deficiency (Figure 7O), indicating that increased Th17 inflammation with DIO was driven by a separate mechanism. Together, these data suggest that the effect of DIO in increasing Th1 responses in female mice was mediated by type I IFN signaling.

DISCUSSION

The incidence of autoimmune diseases has increased over the past half century.[32] In regards to MS, disease risk has increased substantially in those who are obese, carry the MS-related MHC risk haplotype, and are female,[14,33] suggesting an interaction of these host factors in the promotion of Th autoimmunity. Our data revealing a female-predominant increase in Th1 inflammation in humans with obesity and increased type I and type II IFN signaling in murine T cells with DIO provide a mechanistic explanation of how overweightness and obesity may be enhancing autoimmunity in females.

Our finding that type I IFN promoted T cell IFN-γ production and responsiveness by increasing STAT1 expression coincides with a past study of human fibroblasts[34] and provides clarification around the role of type I IFN in promoting Th1 cell differentiation. Early studies demonstrated that IFN-α promotes IFN-γ expression by human T cell blasts[35] by increasing IL-18Rα[36,37] or by inducing STAT4 phosphorylation.[38,39] Then, it was reported that the rise in serum IFN-γ levels seen in mice during lymphocytic choriomeningitis virus infection was dependent on type I IFN and STAT4, but independent of IL-12,[39] thereby framing IFN-α as a cytokine that has similar activities as IL-12 in promoting Th1 cytokine production through STAT4. This notion that IFN-α could promote Th1 differentiation was then dismissed when a series of *in vitro* studies demonstrated that IFN-α treatment could not induce sustained STAT4 phosphorylation or T-bet expression in naive CD4$^+$ T cells.[40–42] Our data rectify this controversy by showing that low-level type I IFN amplifies IFN-γ production by increasing STAT1 activity in T cells. Our findings also coincide with the proposal that sustained low-level type I IFN signaling primes immune cells to make them more poised to respond to infectious challenges.[43]

Our results also add to a growing body of literature describing heightened type I and II IFN signaling and production in females.[44] When compared with males, female monocytes exhibit greater ISG expression,[45,46] and female T cells produce greater

Figure 6. DIO increases type I IFN levels and T cell expression of ISGs and STAT1 in females

(A–C) Naive (CD44$^{low-int}$) CD4$^+$ T cells were isolated from female CTRL or DIO C57BL/6J mice (n = 5 mice/group). Cells were snap frozen or stimulated with anti-CD3/anti-CD28 for 16 h. cDNA was used to probe microarrays.

(A) DAVID GO pathway analysis of top pathways upregulated with DIO (cutoff fold change > 1.5) in activated CD4$^+$ T cells.

(B) Genes upregulated in activated CD4$^+$ T cells with DIO that overlapped with lists of genes enriched in iTreg, Th17, Th2, and Th1 lineage cells.[27]

(C) Venn diagram showing the overlap of DIO-upregulated genes in unstimulated and stimulated CD4$^+$ T cells with those inducible in murine CD4$^+$ T cells in response to type I or type II IFN.[31]

(D–G) Spleen and lymph node cells from C57BL/6J mice fed either a HFD or NCD were stained and gated on naive (CD44$^{low-int}$) CD4$^+$ T cells for total STAT1 (D), IL-18Rα (E), and IL-7Rα (F) or were stimulated *in vitro* with IFN-γ and gMFI, and peak phosphorylated STAT1 (Y701) assessed in naive (CD44$^{low-int}$) CD4$^+$ T cells (G).

(H) Correlation between STAT1 (Y701) gMFI in naive T cells and % body weight change on diets.

(I–K) Serum IFN-γ (I), pan-IFN-α (J), IFN-β (K) levels from female and male CTRL and DIO mice.

(L) Serum IFN-α level in CTRL or DIO female mice, correlated with % weight change on the diets over 4 weeks.

(M) Serum IFN-α levels in female sham or OVX mice after NCD or HFD.

Data points in (D)–(L) are individual mice. Data are presented as mean ± SEM. Significance determined by one-way ANOVA with Tukey's post hoc test with FDR corrected (A and B), or two-way ANOVA with Bonferroni post hoc test (I–K and M), Mann-Whitney test (D–G), or Spearman's test (H and L). *$p \leq 0.05$.

Please cite this article in press as: Cordeiro et al., Obesity intensifies sex-specific interferon signaling to selectively worsen central nervous system autoimmunity in females, Cell Metabolism (2024), https://doi.org/10.1016/j.cmet.2024.07.017

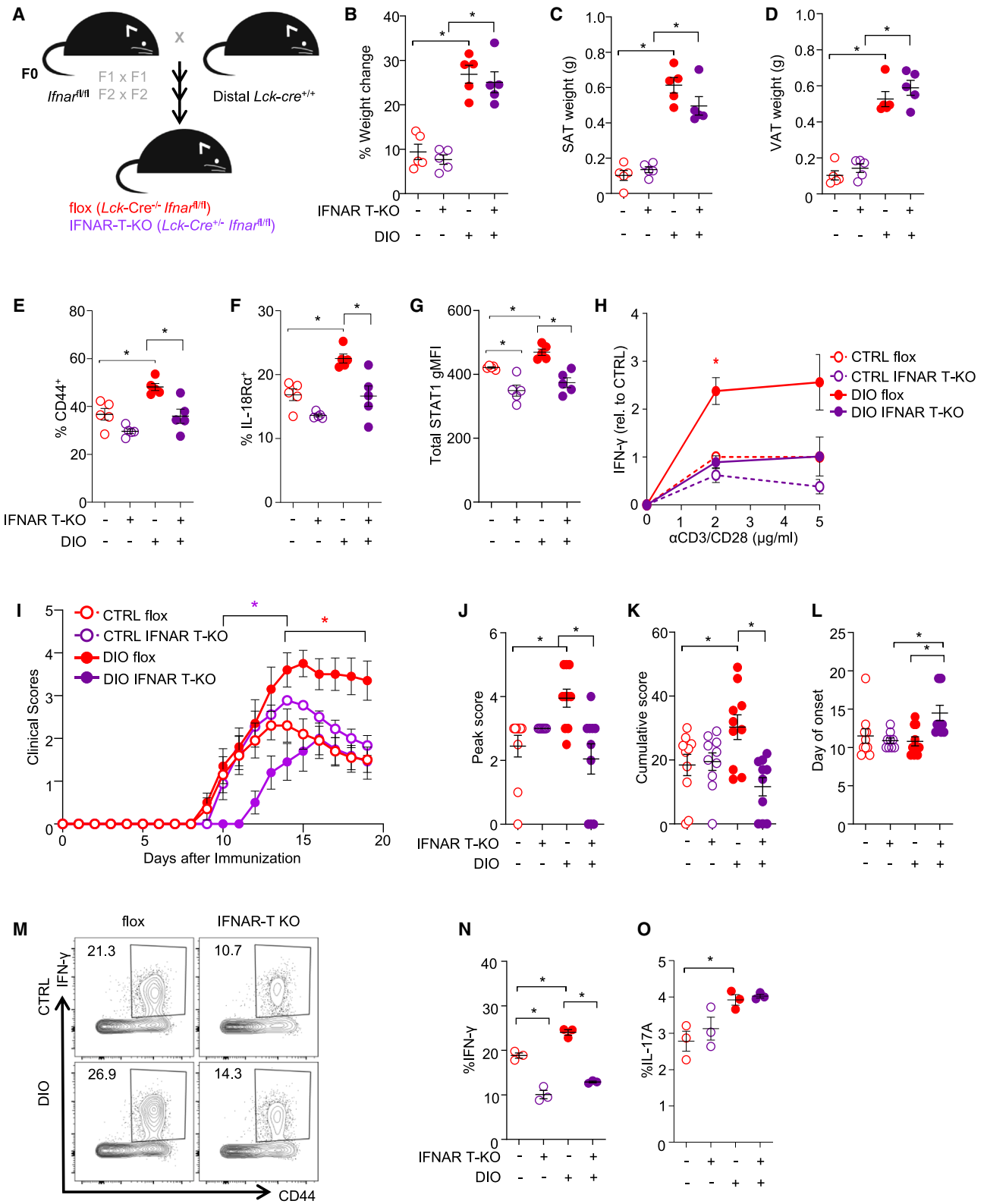

(legend on next page)

Please cite this article in press as: Cordeiro et al., Obesity intensifies sex-specific interferon signaling to selectively worsen central nervous system autoimmunity in females, Cell Metabolism (2024), https://doi.org/10.1016/j.cmet.2024.07.017

CellPress
OPEN ACCESS

levels of IFN-γ.[47,48] In addition, human female plasmacytoid DCs (pDCs) have a greater propensity than male pDCs to secrete type I IFN secretion in response to TLR7 stimulation.[49] These sex differences have been attributed to greater X chromosome gene dosage and estradiol levels in females.[49,50] Our finding that OVX did not lower IFN-α levels in female mice suggested that the female-preponderant effect of DIO in enhancing Th1 inflammation was regulated downstream of IFN-α, at the level of IFN signaling or IFN-γ expression. In this respect, past reports have demonstrated that estradiol enhances T cell IFN-γ expression directly through the binding of the estrogen receptor-α to the *Ifng* promoter[50] or by enhancing STAT4 signaling[51] in $CD4^+$ T cells.

Our findings also coincide with past work describing a role for heightened type I/type II IFN/STAT1 signaling in autoimmunity. Higher IFN-α signaling is a cardinal feature of human systemic lupus erythematosus,[52] and overexpression of IFN-α in lupus-prone NZB/W mice has been shown to promote IgG2a and IgG3 autoantibody production and lupus nephritis via effects in $CD4^+$ T cells.[53] In addition, female mice expressing a human STAT1 gain-of-function mutation exhibit splenomegaly, increased memory T cells, autoantibody development, and spontaneous type I diabetes.[54] It is also reported that ISG expression in immune cells precedes the onset of type I diabetes in human children.[55] Furthermore, mice engineered to have increased IFN-γ levels develop a female-biased spontaneous autoimmune cholangitis that is dependent on IFNAR1 signaling.[56,57] Finally, untreated MS patients exhibit heightened IFN-α-induced STAT1 signaling in immune cells, as compared with healthy controls,[58] and non-responders to IFN-β therapy have higher expression of STAT1 and type I IFN receptor in monocytes.[59]

In conclusion, this study identified a previously unknown interaction between obesity and female sex in enhancing IFN-α levels and promoting Th1 immunity. Thus, BMI and sex should be considered in the design of clinical trials for the treatment of MS and other diseases.

Limitations of the study

Although our studies unraveled how DIO was promoting Th1 immunity in female mice, several questions remain. We still have not pinpointed what tissue or cell is producing IFN-α during DIO. In this respect, past studies reported detecting greater ISG expression and pDC infiltration in the liver with prolonged (16-week) HFD feeding in male mice. It has been speculated that the pDCs may be activated in this and other organs by the release of DNA from dying adipocytes[60] or from increased netosis.[61] In addition, the mechanisms for how DIO is enhancing the expansion of $MOG_{35–55}$-specific T cells during EAE are still not understood. We speculate that this *in vivo* phenotype could be connected with the known role of type I IFNs in promoting the survival of activated $CD4^+$ T cells during clonal expansion in viral infection.[62] Furthermore, our adoptive T cell transfer studies did not distinguish whether the more severe EAE seen in mice transferred with female DIO T cells was due to the increased size of MOG-specific T cell pool or to the individual T cells being more pathogenic. Both could be causal since we observed that female DIO T cells had greater expression of a number of molecules (e.g., T-bet, STAT4, IFN-γ, and GM-CSF) known to promote T cell encephalitogenicity.[63–65] Finally, since DIO and PNO studies were conducted in C57BL/6J mice, a strain that does not exhibit a sex difference in EAE development,[66] we could not study the extent to which the sex difference in type I/II IFN signaling contributed to the sex bias in EAE.

A limitation of our human studies was that serum proteomic measures were conducted on one cohort of individuals at one center, the majority of whom self-identified as White. It is possible that obesity-induced proteomic signatures would vary in individuals of other ethnicities who live in other geographical regions. In addition, our proteomic analysis identified some proteins that were upregulated with obesity in MS patients, but not in controls (e.g., DDX58, IL-12p70, and IL-12Rbeta1). We speculate that increased expression of these proteins in MS could be due to MS-related risk factors including genetic polymorphisms that alter IFN or IL-12 signaling.[67] Notwithstanding, our finding that increased adiposity enhanced T cell IFN-γ secretion in both humans and mice, coupled with similar findings in studies of obese children in the USA, Italy, and Argentina,[68–70] suggests that the effect of obesity in enhancing Th1 inflammation is conserved between humans and mice.

STAR★METHODS

Detailed methods are provided in the online version of this paper and include the following:

- KEY RESOURCES TABLE
- RESOURCE AVAILABILITY
  - Lead contact
  - Materials availability
  - Data and code availability

Figure 7. Loss of IFN-α signaling in female $CD4^+$ T cells negates the effect of DIO on Th1 effector cell responses and EAE

(A) Schematic showing generation of T cell-specific IFNAR1-deficient mice.

(B–D) % body weight change over 4 weeks (B) and SAT (C) and VAT (D) weights at 10 weeks of age.

(E–G) Frequencies of $CD44^+$ (E), IL-18Rα$^+$ (F), and expression of STAT1 (gMFI) (G) in splenic naive $CD4^+$ T cells from CTRL and DIO flox and IFNAR-T-KO mice.

(H) Levels of IFN-γ in culture supernatants at 48 h after *in vitro* stimulation of naive $CD4^+$ T cells with anti-CD3/anti-CD28. Shown is mean ± SEM of fold-change level (relative to flox CTRL) of four independent experiments.

(I–L) Results of EAE studies in CTRL and DIO flox and IFNAR-T-KO mice. EAE clinical scores (I), peak score (J), and cumulative disease score (K) from day 0 to day 19, and day of disease onset (L).

(M–O) Th cell responses in spleens of CTRL and DIO flox and IFNAR-T-KO mice at day 9 post-immunization.

(M) Representative staining of IFN-γ and CD44 in spleen $CD4^+$ T cells.

(N and O) Percentage of splenic $CD4^+$ T cells expressing IFN-γ (N) or IL-17A (O) after PMA/ionomycin stimulation.

Values are mean ± SEM. Data are representative of at least three independent experiments. Significance was determined through two-way ANOVA and Bonferroni post hoc test, *$p \leq 0.05$. Data in (B)–(G), (J)–(L), (N), and (O) are individual mice.

See also Figure S6.

Please cite this article in press as: Cordeiro et al., Obesity intensifies sex-specific interferon signaling to selectively worsen central nervous system autoimmunity in females, Cell Metabolism (2024), https://doi.org/10.1016/j.cmet.2024.07.017

SUPPLEMENTAL INFORMATION

Supplemental information can be found online at https://doi.org/10.1016/j.cmet.2024.07.017.

ACKNOWLEDGMENTS

We thank Danila Leontyev for help with cytokine profiling of mouse serum, Paulina C. Drohomyrecky and Fei Linda Zhao for help with tissue processing, Alexander Luchak and Ken Croitoru for help with extraction of DNA from mouse stool, and Helena Lei for assistance with metabolic assays. This work was supported by a Canadian Institutes of Health Research grant (to S.E.D. and D.A.W.), an MS Canada biomedical discovery grant (to S.E.D.), and National Institutes of Health grants R01AI137047 and R01EY027346 (to R.C.A.). B.C. is supported by a post-doctoral fellowship and J.J.A. by PhD studentship from MS Canada. N.A.-S. is supported by a Keenan post-doctoral fellowship. The graphical abstract was created with BioRender.com.

AUTHOR CONTRIBUTIONS

Conceptualization, S.E.D., R.C.A., B.C., and J.J.A.; data curation, G.P., J.M.G., and K.M.; formal analysis, B.C., J.J.A., C.U., N.A.-S., X.S.R., S.G., S.E.D., and N.S.; funding acquisition, S.E.D., R.C.A., and D.A.W.; investigation, B.C., J.J.A., S.G., C.U., N.A.-S., and S.E.D.; resources, S.E.D., G.P., J.M.G., D.G.B., D.A.W., and K.M.; supervision, S.E.D. and R.C.A.; visualization, B.C., J.J.A., S.E.D., and R.C.A.; writing – original draft, S.E.D., B.C., J.J.A., and R.C.A.; writing – review & editing, all authors.

DECLARATION OF INTERESTS

J.J.A. is currently an employee of Bristol Myers Squibb. R.C.A. is on the advisory board for Progentec Diagnostics Inc.

Received: January 5, 2024
Revised: April 29, 2024
Accepted: July 23, 2024
Published: August 20, 2024

REFERENCES

1. Reich, D.S., Lucchinetti, C.F., and Calabresi, P.A. (2018). Multiple sclerosis. N. Engl. J. Med. *378*, 169–180. https://doi.org/10.1056/NEJMra1401483.
2. Dendrou, C.A., Fugger, L., and Friese, M.A. (2015). Immunopathology of multiple sclerosis. Nat. Rev. Immunol. *15*, 545–558. https://doi.org/10.1038/nri3871.
3. Rasouli, J., Ciric, B., Imitola, J., Gonnella, P., Hwang, D., Mahajan, K., Mari, E.R., Safavi, F., Leist, T.P., Zhang, G.X., et al. (2015). Expression of GM-CSF in T cells is increased in multiple sclerosis and suppressed by IFN-beta therapy. J. Immunol. *194*, 5085–5093. https://doi.org/10.4049/jimmunol.1403243.
4. McGinley, M.P., Goldschmidt, C.H., and Rae-Grant, A.D. (2021). Diagnosis and treatment of multiple sclerosis: a review. JAMA *325*, 765–779. https://doi.org/10.1001/jama.2020.26858.
5. Rangachari, M., and Kuchroo, V.K. (2013). Using EAE to better understand principles of immune function and autoimmune pathology. J. Autoimmun. *45*, 31–39. https://doi.org/10.1016/j.jaut.2013.06.008.
6. Krishnarajah, S., and Becher, B. (2022). T(H) cells and cytokines in encephalitogenic disorders. Front. Immunol. *13*, 822919. https://doi.org/10.3389/fimmu.2022.822919.
7. Hirota, K., Duarte, J.H., Veldhoen, M., Hornsby, E., Li, Y., Cua, D.J., Ahlfors, H., Wilhelm, C., Tolaini, M., Menzel, U., et al. (2011). Fate mapping of IL-17-producing T cells in inflammatory responses. Nat. Immunol. *12*, 255–263. https://doi.org/10.1038/ni.1993.
8. Duhen, R., Glatigny, S., Arbelaez, C.A., Blair, T.C., Oukka, M., and Bettelli, E. (2013). Cutting edge: the pathogenicity of IFN-gamma-producing Th17 cells is independent of T-bet. J. Immunol. *190*, 4478–4482. https://doi.org/10.4049/jimmunol.1203172.
9. Alfredsson, L., and Olsson, T. (2019). Lifestyle and environmental factors in multiple sclerosis. Cold Spring Harb. Perspect. Med. *9*, a028944. https://doi.org/10.1101/cshperspect.a028944.
10. Alvarez-Sanchez, N., and Dunn, S.E. (2023). Immune cell contributors to the female sex bias in multiple sclerosis and experimental autoimmune encephalomyelitis. Curr. Top. Behav. Neurosci. *62*, 333–373. https://doi.org/10.1007/7854_2022_324.
11. Koch-Henriksen, N., and Sørensen, P.S. (2010). The changing demographic pattern of multiple sclerosis epidemiology. Lancet Neurol. *9*, 520–532. https://doi.org/10.1016/S1474-4422(10)70064-8.
12. Orton, S.M., Herrera, B.M., Yee, I.M., Valdar, W., Ramagopalan, S.V., Sadovnick, A.D., and Ebers, G.C.; Canadian Collaborative Study Group (2006). Sex ratio of multiple sclerosis in Canada: a longitudinal study. Lancet Neurol. *5*, 932–936. https://doi.org/10.1016/S1474-4422(06)70581-6.
13. Versini, M., Jeandel, P.Y., Rosenthal, E., and Shoenfeld, Y. (2014). Obesity in autoimmune diseases: not a passive bystander. Autoimmun. Rev. *13*, 981–1000. https://doi.org/10.1016/j.autrev.2014.07.001.
14. Hedström, A.K., Lima Bomfim, I., Barcellos, L., Gianfrancesco, M., Schaefer, C., Kockum, I., Olsson, T., and Alfredsson, L. (2014). Interaction between adolescent obesity and HLA risk genes in the etiology of multiple sclerosis. Neurology *82*, 865–872. https://doi.org/10.1212/WNL.0000000000000203.
15. Daniel, H., Gholami, A.M., Berry, D., Desmarchelier, C., Hahne, H., Loh, G., Mondot, S., Lepage, P., Rothballer, M., Walker, A., et al. (2014). High-fat diet alters gut microbiota physiology in mice. ISME J. *8*, 295–308. https://doi.org/10.1038/ismej.2013.155.
16. Shahi, S.K., Ghimire, S., Lehman, P., and Mangalam, A.K. (2022). Obesity induced gut dysbiosis contributes to disease severity in an animal model of multiple sclerosis. Front. Immunol. *13*, 966417. https://doi.org/10.3389/fimmu.2022.966417.
17. West, D.B., Boozer, C.N., Moody, D.L., and Atkinson, R.L. (1992). Dietary obesity in nine inbred mouse strains. Am. J. Physiol. *262*, R1025–R1032. https://doi.org/10.1152/ajpregu.1992.262.6.R1025.

Please cite this article in press as: Cordeiro et al., Obesity intensifies sex-specific interferon signaling to selectively worsen central nervous system autoimmunity in females, Cell Metabolism (2024), https://doi.org/10.1016/j.cmet.2024.07.017

CellPress
OPEN ACCESS

18. Chadt, A., Leicht, K., Deshmukh, A., Jiang, L.Q., Scherneck, S., Bernhardt, U., Dreja, T., Vogel, H., Schmolz, K., Kluge, R., et al. (2008). Tbc1d1 mutation in lean mouse strain confers leanness and protects from diet-induced obesity. Nat. Genet. *40*, 1354–1359. https://doi.org/10.1038/ng.244.

19. Parra-Vargas, M., Ramon-Krauel, M., Lerin, C., and Jimenez-Chillaron, J.C. (2020). Size does matter: litter size strongly determines adult metabolism in rodents. Cell Metab. *32*, 334–340. https://doi.org/10.1016/j.cmet.2020.07.014.

20. Schulz, E.G., Mariani, L., Radbruch, A., and Höfer, T. (2009). Sequential polarization and imprinting of type 1 T helper lymphocytes by interferon-gamma and interleukin-12. Immunity *30*, 673–683. https://doi.org/10.1016/j.immuni.2009.03.013.

21. Afkarian, M., Sedy, J.R., Yang, J., Jacobson, N.G., Cereb, N., Yang, S.Y., Murphy, T.L., and Murphy, K.M. (2002). T-bet is a STAT1-induced regulator of IL-12R expression in naive CD4+ T cells. Nat. Immunol. *3*, 549–557. https://doi.org/10.1038/ni794.

22. Rogers, N.H., Perfield, J.W., 2nd, Strissel, K.J., Obin, M.S., and Greenberg, A.S. (2009). Reduced energy expenditure and increased inflammation are early events in the development of ovariectomy-induced obesity. Endocrinology *150*, 2161–2168. https://doi.org/10.1210/en.2008-1405.

23. Matarese, G. (2023). The link between obesity and autoimmunity. Science *379*, 1298–1300. https://doi.org/10.1126/science.ade0113.

24. Nyirenda, M.H., Fadda, G., Healy, L.M., Mexhitaj, I., Poliquin-Lasnier, L., Hanwell, H., Saveriano, A.W., Rozenberg, A., Li, R., Moore, C.S., et al. (2021). Pro-inflammatory adiponectin in pediatric-onset multiple sclerosis. Mult. Scler. *27*, 1948–1959. https://doi.org/10.1177/1352458521989090.

25. Marrodan, M., Farez, M.F., Balbuena Aguirre, M.E., and Correale, J. (2021). Obesity and the risk of multiple sclerosis. The role of leptin. Ann. Clin. Transl. Neurol. *8*, 406–424. https://doi.org/10.1002/acn3.51291.

26. Matarese, G., Sanna, V., Di Giacomo, A., Lord, G.M., Howard, J.K., Bloom, S.R., Lechler, R.I., Fontana, S., and Zappacosta, S. (2001). Leptin potentiates experimental autoimmune encephalomyelitis in SJL female mice and confers susceptibility to males. Eur. J. Immunol. *31*, 1324–1332. https://doi.org/10.1002/1521-4141(200105)31:5<1324::AID-IMMU1324>3.0.CO;2-Y.

27. Wei, G., Abraham, B.J., Yagi, R., Jothi, R., Cui, K., Sharma, S., Narlikar, L., Northrup, D.L., Tang, Q., Paul, W.E., et al. (2011). Genome-wide analyses of transcription factor GATA3-mediated gene regulation in distinct T cell types. Immunity *35*, 299–311. https://doi.org/10.1016/j.immuni.2011.08.007.

28. Hoshino, K., Tsutsui, H., Kawai, T., Takeda, K., Nakanishi, K., Takeda, Y., and Akira, S. (1999). Cutting edge: generation of IL-18 receptor-deficient mice: evidence for IL-1 receptor-related protein as an essential IL-18 binding receptor. J. Immunol. *162*, 5041–5044. https://doi.org/10.4049/jimmunol.162.9.5041.

29. Takeda, K., Tsutsui, H., Yoshimoto, T., Adachi, O., Yoshida, N., Kishimoto, T., Okamura, H., Nakanishi, K., and Akira, S. (1998). Defective NK cell activity and Th1 response in IL-18–deficient mice. Immunity *8*, 383–390. https://doi.org/10.1016/s1074-7613(00)80543-9.

30. Lee, L.F., Axtell, R., Tu, G.H., Logronio, K., Dilley, J., Yu, J., Rickert, M., Han, B., Evering, W., Walker, M.G., et al. (2011). IL-7 promotes T(H)1 development and serum IL-7 predicts clinical response to interferon-β in multiple sclerosis. Sci. Transl. Med. *3*, 93ra68. https://doi.org/10.1126/scitranslmed.3002400.

31. Mostafavi, S., Yoshida, H., Moodley, D., LeBoité, H., Rothamel, K., Raj, T., Ye, C.J., Chevrier, N., Zhang, S.Y., Feng, T., et al. (2016). Parsing the interferon transcriptional network and its disease associations. Cell *164*, 564–578. https://doi.org/10.1016/j.cell.2015.12.032.

32. Miller, F.W. (2023). The increasing prevalence of autoimmunity and autoimmune diseases: an urgent call to action for improved understanding, diagnosis, treatment, and prevention. Curr. Opin. Immunol. *80*, 102266. https://doi.org/10.1016/j.coi.2022.102266.

33. Rasul, T., and Frederiksen, J.L. (2018). Link between overweight/obese in children and youngsters and occurrence of multiple sclerosis. J. Neurol. *265*, 2755–2763. https://doi.org/10.1007/s00415-018-8869-9.

34. Gough, D.J., Messina, N.L., Hii, L., Gould, J.A., Sabapathy, K., Robertson, A.P.S., Trapani, J.A., Levy, D.E., Hertzog, P.J., Clarke, C.J.P., et al. (2010). Functional crosstalk between type I and II interferon through the regulated expression of STAT1. PLoS Biol. *8*, e1000361. https://doi.org/10.1371/journal.pbio.1000361.

35. Brinkmann, V., Geiger, T., Alkan, S., and Heusser, C.H. (1993). Interferon alpha increases the frequency of interferon gamma-producing human CD4+ T cells. J. Exp. Med. *178*, 1655–1663. https://doi.org/10.1084/jem.178.5.1655.

36. Sareneva, T., Matikainen, S., Kurimoto, M., and Julkunen, I. (1998). Influenza A virus-induced IFN-alpha/beta and IL-18 synergistically enhance IFN-gamma gene expression in human T cells. J. Immunol. *160*, 6032–6038. https://doi.org/10.4049/jimmunol.160.12.6032.

37. Sareneva, T., Julkunen, I., and Matikainen, S. (2000). IFN-alpha and IL-12 induce IL-18 receptor gene expression in human NK and T cells. J. Immunol. *165*, 1933–1938. https://doi.org/10.4049/jimmunol.165.4.1933.

38. Cho, S.S., Bacon, C.M., Sudarshan, C., Rees, R.C., Finbloom, D., Pine, R., and O'Shea, J.J. (1996). Activation of STAT4 by IL-12 and IFN-alpha: evidence for the involvement of ligand-induced tyrosine and serine phosphorylation. J. Immunol. *157*, 4781–4789. https://doi.org/10.4049/jimmunol.157.11.4781.

39. Nguyen, K.B., Watford, W.T., Salomon, R., Hofmann, S.R., Pien, G.C., Morinobu, A., Gadina, M., O'Shea, J.J., and Biron, C.A. (2002). Critical role for STAT4 activation by type 1 interferons in the interferon-gamma response to viral infection. Science *297*, 2063–2066. https://doi.org/10.1126/science.1074900.

40. Athie-Morales, V., Smits, H.H., Cantrell, D.A., and Hilkens, C.M.U. (2004). Sustained IL-12 signaling is required for Th1 development. J. Immunol. *172*, 61–69. https://doi.org/10.4049/jimmunol.172.1.61.

41. Berenson, L.S., Farrar, J.D., Murphy, T.L., and Murphy, K.M. (2004). Frontline: absence of functional STAT4 activation despite detectable tyrosine phosphorylation induced by murine IFN-alpha. Eur. J. Immunol. *34*, 2365–2374. https://doi.org/10.1002/eji.200324829.

42. Ramos, H.J., Davis, A.M., George, T.C., and Farrar, J.D. (2007). IFN-alpha is not sufficient to drive Th1 development due to lack of stable T-bet expression. J. Immunol. *179*, 3792–3803. https://doi.org/10.4049/jimmunol.179.6.3792.

43. Gough, D.J., Messina, N.L., Clarke, C.J.P., Johnstone, R.W., and Levy, D.E. (2012). Constitutive type I interferon modulates homeostatic balance through tonic signaling. Immunity *36*, 166–174. https://doi.org/10.1016/j.immuni.2012.01.011.

44. Dunn, S.E., Perry, W.A., and Klein, S.L. (2024). Mechanisms and consequences of sex differences in immune responses. Nat. Rev. Nephrol. *20*, 37–55. https://doi.org/10.1038/s41581-023-00787-w.

45. Gal-Oz, S.T., Maier, B., Yoshida, H., Seddu, K., Elbaz, N., Czysz, C., Zuk, O., Stranger, B.E., Ner-Gaon, H., and Shay, T. (2019). ImmGen report: sexual dimorphism in the immune system transcriptome. Nat. Commun. *10*, 4295. https://doi.org/10.1038/s41467-019-12348-6.

46. Schmiedel, B.J., Singh, D., Madrigal, A., Valdovino-Gonzalez, A.G., White, B.M., Zapardiel-Gonzalo, J., Ha, B., Altay, G., Greenbaum, J.A., McVicker, G., et al. (2018). Impact of genetic polymorphisms on human immune cell gene expression. Cell *175*, 1701–1715.e16. https://doi.org/10.1016/j.cell.2018.10.022.

47. Zhang, M.A., Moshkova, M., Kebir, M., Chruscinski, A., Nguyen, H., Akkermann, R., Stancyk, F.Z., Prat, A., Steinman, L., and Dunn, S.E. (2012). Peroxisome proliferator-activated receptor (PPAR)alpha and -gamma regulate IFN-gamma and IL-17A production by human T cells in a sex-specific way. Proc. Natl. Acad. Sci. USA *109*, 9505–9510. https://doi.org/10.1073/pnas.1118458109.

48. Dunn, S.E., Ousman, S.S., Sobel, R.A., Zuniga, L., Baranzini, S.E., Youssef, S., Crowell, A., Loh, J., Oksenberg, J., and Steinman, L. (2007).

Please cite this article in press as: Cordeiro et al., Obesity intensifies sex-specific interferon signaling to selectively worsen central nervous system autoimmunity in females, Cell Metabolism (2024), https://doi.org/10.1016/j.cmet.2024.07.017

Peroxisome proliferator-activated receptor (PPAR)alpha expression in T cells mediates gender differences in development of T cell-mediated autoimmunity. J. Exp. Med. *204*, 321–330. https://doi.org/10.1084/jem.20061839.

49. Seillet, C., Laffont, S., Trémollières, F., Rouquié, N., Ribot, C., Arnal, J.F., Douin-Echinard, V., Gourdy, P., and Guéry, J.C. (2012). The TLR-mediated response of plasmacytoid dendritic cells is positively regulated by estradiol in vivo through cell-intrinsic estrogen receptor alpha signaling. Blood *119*, 454–464. https://doi.org/10.1182/blood-2011-08-371831.
50. Fox, H.S., Bond, B.L., and Parslow, T.G. (1991). Estrogen regulates the IFN-gamma promoter. J. Immunol. *146*, 4362–4367. https://doi.org/10.4049/jimmunol.146.12.4362.
51. Bao, M., Yang, Y., Jun, H.S., and Yoon, J.W. (2002). Molecular mechanisms for gender differences in susceptibility to T cell-mediated autoimmune diabetes in nonobese diabetic mice. J. Immunol. *168*, 5369–5375. https://doi.org/10.4049/jimmunol.168.10.5369.
52. Crow, M.K., Olferiev, M., and Kirou, K.A. (2019). Type I interferons in autoimmune disease. Annu. Rev. Pathol. *14*, 369–393. https://doi.org/10.1146/annurev-pathol-020117-043952.
53. Liu, Z., Bethunaickan, R., Huang, W., Lodhi, U., Solano, I., Madaio, M.P., and Davidson, A. (2011). Interferon-alpha accelerates murine systemic lupus erythematosus in a T cell-dependent manner. Arthritis Rheum. *63*, 219–229. https://doi.org/10.1002/art.30087.
54. Scott, O., Visuvanathan, S., Reddy, E., Mahamed, D., Gu, B., Roifman, C.M., Cohn, R.D., Guidos, C.J., and Ivakine, E.A. (2023). The human Stat1 gain-of-function T385M mutation causes expansion of activated T-follicular helper/T-helper 1-like CD4 T cells and sex-biased autoimmunity in specific pathogen-free mice. Front. Immunol. *14*, 1183273. https://doi.org/10.3389/fimmu.2023.1183273.
55. Ferreira, R.C., Guo, H., Coulson, R.M.R., Smyth, D.J., Pekalski, M.L., Burren, O.S., Cutler, A.J., Doecke, J.D., Flint, S., McKinney, E.F., et al. (2014). A type I interferon transcriptional signature precedes autoimmunity in children genetically at risk for type 1 diabetes. Diabetes *63*, 2538–2550. https://doi.org/10.2337/db13-1777.
56. Bae, H.R., Leung, P.S.C., Tsuneyama, K., Valencia, J.C., Hodge, D.L., Kim, S., Back, T., Karwan, M., Merchant, A.S., Baba, N., et al. (2016). Chronic expression of interferon-gamma leads to murine autoimmune cholangitis with a female predominance. Hepatology *64*, 1189–1201. https://doi.org/10.1002/hep.28641.
57. Bae, H.R., Hodge, D.L., Yang, G.X., Leung, P.S.C., Chodisetti, S.B., Valencia, J.C., Sanford, M., Fenimore, J.M., Rahman, Z.S.M., Tsuneyama, K., et al. (2018). The interplay of type I and type II interferons in murine autoimmune cholangitis as a basis for sex-biased autoimmunity. Hepatology *67*, 1408–1419. https://doi.org/10.1002/hep.29524.
58. Canto, E., Isobe, N., Didonna, A., MS-EPIC Study Group, Hauser, S.L., and Oksenberg, J.R. (2018). Aberrant STAT phosphorylation signaling in peripheral blood mononuclear cells from multiple sclerosis patients. J. Neuroinflammation *15*, 72. https://doi.org/10.1186/s12974-018-1105-9.
59. Hegen, H., Adrianto, I., Lessard, C.J., Millonig, A., Bertolotto, A., Comabella, M., Giovannoni, G., Guger, M., Hoelzl, M., Khalil, M., et al. (2016). Cytokine profiles show heterogeneity of interferon-beta response in multiple sclerosis patients. Neurol. Neuroimmunol. Neuroinflamm. *3*, e202. https://doi.org/10.1212/NXI.0000000000000202.
60. Nishimoto, S., Fukuda, D., Higashikuni, Y., Tanaka, K., Hirata, Y., Murata, C., Kim-Kaneyama, J.R., Sato, F., Bando, M., Yagi, S., et al. (2016). Obesity-induced DNA released from adipocytes stimulates chronic adipose tissue inflammation and insulin resistance. Sci. Adv. *2*, e1501332. https://doi.org/10.1126/sciadv.1501332.
61. Revelo, X.S., Ghazarian, M., Chng, M.H.Y., Luck, H., Kim, J.H., Zeng, K., Shi, S.Y., Tsai, S., Lei, H., Kenkel, J., et al. (2016). Nucleic acid-targeting pathways promote inflammation in obesity-related insulin resistance. Cell Rep. *16*, 717–730. https://doi.org/10.1016/j.celrep.2016.06.024.
62. Havenar-Daughton, C., Kolumam, G.A., and Murali-Krishna, K. (2006). Cutting Edge: the direct action of type I IFN on CD4 T cells is critical for sustaining clonal expansion in response to a viral but not a bacterial infection. J. Immunol. *176*, 3315–3319. https://doi.org/10.4049/jimmunol.176.6.3315.
63. Lee, P.W., Smith, A.J., Yang, Y., Selhorst, A.J., Liu, Y., Racke, M.K., and Lovett-Racke, A.E. (2017). IL-23R-activated STAT3/STAT4 is essential for Th1/Th17-mediated CNS autoimmunity. JCI Insight *2*, e91663. https://doi.org/10.1172/jci.insight.91663.
64. Buzzelli, A.A., McWilliams, I.L., Shin, B., Bryars, M.T., and Harrington, L.E. (2023). Intrinsic STAT4 expression controls effector CD4 T cell migration and Th17 pathogenicity. J. Immunol. *210*, 1667–1676. https://doi.org/10.4049/jimmunol.2200606.
65. Yang, Y., Weiner, J., Liu, Y., Smith, A.J., Huss, D.J., Winger, R., Peng, H., Cravens, P.D., Racke, M.K., and Lovett-Racke, A.E. (2009). T-bet is essential for encephalitogenicity of both Th1 and Th17 cells. J. Exp. Med. *206*, 1549–1564. https://doi.org/10.1084/jem.20082584.
66. Papenfuss, T.L., Rogers, C.J., Gienapp, I., Yurrita, M., McClain, M., Damico, N., Valo, J., Song, F., and Whitacre, C.C. (2004). Sex differences in experimental autoimmune encephalomyelitis in multiple murine strains. J. Neuroimmunol. *150*, 59–69. https://doi.org/10.1016/j.jneuroim.2004.01.018.
67. International; Multiple; Sclerosis; Genetics Consortium (2019). Multiple sclerosis genomic map implicates peripheral immune cells and microglia in susceptibility. Science *365*, eaav7188. https://doi.org/10.1126/science.aav7188.
68. Inzaugarat, M.E., Billordo, L.A., Vodánovich, F., Cervini, G.M., Casavalle, P.L., Vedire, C., and Cherñavsky, A.C. (2014). Alterations in innate and adaptive immune leukocytes are involved in paediatric obesity. Pediatr. Obes. *9*, 381–390. https://doi.org/10.1111/j.2047-6310.2013.00179.x.
69. Pacifico, L., Di Renzo, L., Anania, C., Osborn, J.F., Ippoliti, F., Schiavo, E., and Chiesa, C. (2006). Increased T-helper interferon-gamma-secreting cells in obese children. Eur. J. Endocrinol. *154*, 691–697. https://doi.org/10.1530/eje.1.02138.
70. Rastogi, D., Canfield, S.M., Andrade, A., Isasi, C.R., Hall, C.B., Rubinstein, A., and Arens, R. (2012). Obesity-associated asthma in children: a distinct entity. Chest *141*, 895–905. https://doi.org/10.1378/chest.11-0930.
71. Polman, C.H., Reingold, S.C., Banwell, B., Clanet, M., Cohen, J.A., Filippi, M., Fujihara, K., Havrdova, E., Hutchinson, M., Kappos, L., et al. (2011). Diagnostic criteria for multiple sclerosis: 2010 revisions to the McDonald criteria. Ann. Neurol. *69*, 292–302. https://doi.org/10.1002/ana.22366.
72. Thompson, A.J., Banwell, B.L., Barkhof, F., Carroll, W.M., Coetzee, T., Comi, G., Correale, J., Fazekas, F., Filippi, M., Freedman, M.S., et al. (2018). Diagnosis of multiple sclerosis: 2017 revisions of the McDonald criteria. Lancet Neurol. *17*, 162–173. https://doi.org/10.1016/S1474-4422(17)30470-2.
73. Zhang, D.J., Wang, Q., Wei, J., Baimukanova, G., Buchholz, F., Stewart, A.F., Mao, X., and Killeen, N. (2005). Selective expression of the Cre recombinase in late-stage thymocytes using the distal promoter of the Lck gene. J. Immunol. *174*, 6725–6731. https://doi.org/10.4049/jimmunol.174.11.6725.
74. Drohomyrecky, P.C., Doroshenko, E.R., Akkermann, R., Moshkova, M., Yi, T.J., Zhao, F.L., Ahn, J.J., McGaha, T.L., Pahan, K., and Dunn, S.E. (2019). Peroxisome proliferator-activated receptor-δ acts within peripheral myeloid cells to limit Th cell priming during experimental autoimmune encephalomyelitis. J. Immunol. *203*, 2588–2601. https://doi.org/10.4049/jimmunol.1801200.
75. Doroshenko, E.R., Drohomyrecky, P.C., Gower, A., Whetstone, H., Cahill, L.S., Ganguly, M., Spring, S., Yi, T.J., Sled, J.G., and Dunn, S.E. (2021). Peroxisome proliferator-activated receptor-delta deficiency in microglia results in exacerbated axonal injury and tissue loss in experimental autoimmune encephalomyelitis. Front. Immunol. *12*, 570425. https://doi.org/10.3389/fimmu.2021.570425.
76. Caporaso, J.G., Lauber, C.L., Walters, W.A., Berg-Lyons, D., Huntley, J., Fierer, N., Owens, S.M., Betley, J., Fraser, L., Bauer, M., et al. (2012). Ultra-high-throughput microbial community analysis on the Illumina

Please cite this article in press as: Cordeiro et al., Obesity intensifies sex-specific interferon signaling to selectively worsen central nervous system autoimmunity in females, Cell Metabolism (2024), https://doi.org/10.1016/j.cmet.2024.07.017

HiSeq and MiSeq platforms. ISME J. *6*, 1621–1624. https://doi.org/10.1038/ismej.2012.8.

77. Bolyen, E., Rideout, J.R., Dillon, M.R., Bokulich, N.A., Abnet, C.C., Al-Ghalith, G.A., Alexander, H., Alm, E.J., Arumugam, M., Asnicar, F., et al. (2019). Reproducible, interactive, scalable and extensible microbiome data science using QIIME 2. Nat. Biotechnol. *37*, 852–857. https://doi.org/10.1038/s41587-019-0209-9.

78. Cahill, L.S., Zhang, M.A., Ramaglia, V., Whetstone, H., Sabbagh, M.P., Yi, T.J., Woo, L., Przybycien, T.S., Moshkova, M., Zhao, F.L., et al. (2019). Aged hind-limb clasping experimental autoimmune encephalomyelitis models aspects of the neurodegenerative process seen in multiple sclerosis. Proc. Natl. Acad. Sci. USA *116*, 22710–22720. https://doi.org/10.1073/pnas.1915141116.

79. Ucciferri, C.C., Gower, A., Alvarez-Sanchez, N., Whetstone, H., Ramaglia, V., Gommerman, J.L., Brand-Arzamendi, K., Schneider, R., and Dunn, S.E. (2024). Scoring central nervous system inflammation, demyelination, and axon injury in experimental autoimmune encephalomyelitis. J. Vis. Exp. https://doi.org/10.3791/65738.

80. Dunn, S.E., Bhat, R., Straus, D.S., Sobel, R.A., Axtell, R., Johnson, A., Nguyen, K., Mukundan, L., Moshkova, M., Dugas, J.C., et al. (2010). Peroxisome proliferator-activated receptor delta limits the expansion of pathogenic Th cells during central nervous system autoimmunity. J. Exp. Med. *207*, 1599–1608. https://doi.org/10.1084/jem.20091663.

Please cite this article in press as: Cordeiro et al., Obesity intensifies sex-specific interferon signaling to selectively worsen central nervous system autoimmunity in females, Cell Metabolism (2024), https://doi.org/10.1016/j.cmet.2024.07.017

STAR★METHODS

KEY RESOURCES TABLE

REAGENT or RESOURCE	SOURCE	IDENTIFIER
Antibodies		
CD16/CD32 (93)	Biolegend	Biolegend Cat# 101301; RRID: AB_312800
APC-CD3 (145-2C11)	Biolegend	Biolegend: Cat# 100312; RRID: AB_312677
FITC-CD3 (145-2C11)	Biolegend	Biolegend: Cat# 100306; RRID: AB_312671
FITC-CD4 (GK1.5)	Biolegend	Biolegend: Cat# 100406; RRID: AB_312690
PE-Cy7-CD4 (RM4-5)	Biolegend	Biolegend: Cat# 100528; RRID: AB_312729
PE-Cy5-CD8 (53-6.7)	Biolegend	Biolegend Cat# 100710; RRID: AB_312749
PE-CD11b (M1/70)	Biolegend	Biolegend Cat# 101208; RRID: AB_312791
APC-CD11b (M1/70)	Biolegend	Biolegend Cat# 101212; RRID: AB_312795
APC-CD11c (HL3)	BD	BD Cat# 550261; RRID: AB_398460
BV421-CD19 (B4)	BD	BD Cat# 562441; RRID: AB_11154587
PE-CD25 (PC61.5)	Biolegend	BioLegend Cat# 102007; RRID: AB_312856
APC-CD25 (PC61.5)	Biolegend	BioLegend Cat# 102011; RRID: AB_312860
FITC-CD44 (IM7)	Biolegend	BioLegend Cat# 103022; RRID: AB_493685
PE-CD44 (IM7)	Biolegend	BioLegend Cat# 103024; RRID: AB_493687
PE-Cy5-CD44 (IM7)	Biolegend	BioLegend Cat# 103009; RRID: AB_312960
PE-Cy7-CD44 (IM7)	Biolegend	BioLegend Cat# 103029; RRID: AB_830786
Alexa fluor700-CD44 (IM7)	BD	BD Biosciences Cat# 560567; RRID: AB_1727480
PE-Cy7 CD45 (30-F11)	Biolegend	BioLegend Cat# 103114; RRID: AB_312979
PE-CD45.1 (A20)	Biolegend	BD Biosciences Cat# 561872; RRID: AB_10897174
PE-Cy7 CD45.1 (A20)	Biolegend	BioLegend Cat# 110730 (also 110729); RRID: AB_1134168
FITC-CD45.2 (104)	Biolegend	BioLegend Cat# 109805; RRID: AB_313442
PE-IFNAR1 (MAR1-5A3)	Thermofisher	Thermo Fisher Scientific Cat# 12-5945-82; RRID: AB_2572646
PE-IFNGR1 (GIR-208)	Thermofisher	Thermo Fisher Scientific Cat# 12-1199-42; RRID: AB_11150056
eFluor450- IL-18Ra (P3TUNYA)	Thermofisher	Thermo Fisher Scientific Cat# 48-5183-82; RRID: AB_2574069
FITC-Ly6G (1A8)	Biolegend	BioLegend Cat# 127605 (also 127606); RRID: AB_1236488
PE-Vβ11 TCR (RR3-15)	Thermofisher	Thermo Fisher Scientific Cat# 12-5827-82; RRID: AB_2762684
SB600-NK1.1 (PK136)	Thermofisher	Thermo Fisher Scientific Cat# 63-5941-82; RRID: AB_2637451
PE-FOXP3 (FJK-16s)	Thermofisher	Thermo Fisher Scientific Cat# 12-5773-82; RRID: AB_465936
Alexa488-FOXP3 (MF-14)	Biolegend	BioLegend Cat# 126406; RRID: AB_1089113
FITC-GM-CSF (MP1-22E9)	Biolegend	BioLegend Cat# 505404; RRID: AB_315380
PE-IFN-γ (XMG1.2)	Biolegend	BioLegend Cat# 505807; RRID: AB_315401
APC-IFN-γ (XMG1.2)	Biolegend	BioLegend Cat# 505810; RRID: AB_315404
APC-IL-17A (eBio17B7)	Thermofisher	Thermo Fisher Scientific Cat# 17-7177-81; RRID: AB_763580

(*Continued on next page*)

Please cite this article in press as: Cordeiro et al., Obesity intensifies sex-specific interferon signaling to selectively worsen central nervous system autoimmunity in females, Cell Metabolism (2024), https://doi.org/10.1016/j.cmet.2024.07.017

CellPress
OPEN ACCESS

Continued

REAGENT or RESOURCE	SOURCE	IDENTIFIER
PE-IL-17A (eBio17B7)	Thermofisher	Thermo Fisher Scientific Cat# 12-7177-81; RRID: AB_763582
APC-MOG38-49 variant S45D tetramer	NIH Tetramer Core Facility	N/A
APC-human CLIP87-101 I-Ab tetramer	NIH Tetramer Core Facility	N/A
anti-Stat1 pY701-Alex Fluor 647 (4a)	BD	BD Biosciences Cat# 612597; RRID: AB_399880
Anti-Total STAT1 Alex Fluor 647 (1/Stat1)	BD	BD Biosciences Cat# 558560; RRID: AB_647143
IL-7Rα PE-Cy7 (A7R34)	Biolegend	Biolegend Cat# 135013; RRID: AB_1937265
CD4-APC-eF780 (GK1.5)	Thermofisher	Thermo Fisher Scientific Cat# 47-0041-82; RRID: AB_11218896
CD8-FITC (53–6.7)	Biolegend	BioLegend Cat# 100705 (also 100706); RRID: AB_312744
Vβ11-PE (RR3-15)	Biolegend	BioLegend Cat# 139003; RRID: AB_10613472
CD28 Monoclonal Antibody (37.51)	Thermofisher	Thermo Fisher Scientific Cat# 16-0281-38; RRID: AB_2865680
CD3 Monoclonal Antibody (145-2C11)	Thermofisher	Thermo Fisher Scientific Cat# 16-0031-38; RRID: AB_2865575
Biotin-IFNAR (MAR1-5A3)	Biolegend	BioLegend Cat# 127306; RRID: AB_1134249
Biological samples		
Human serum (O-link analysis)	Arthritis and Clinical Immunology Research Program, Oklahoma Medical Research Foundation	IRB# 16-05
Peripheral blood mononuclear cells	University Health Network and Stanford University	REB 09-0577-AE IRB# 97959
Chemicals, peptides, and recombinant proteins		
MOG35-55 peptide MEVGWYRSPFSRVVHLYRNGK	Genemed Synthesis	Genemed Synthesis Cat#: MOG3555-P2-5
PLP139-151 peptide HSLGKWLGHPDKF	Genemed Synthesis	Genemed Synthesis Cat#: SP-86876-5
heat-killed Mycobacterium tuberculosis H37Ra	Difco Laboratories	Difco Laboratories Cat#: DF3114-33-8
Bordetella pertussis toxin	List Biologicals	List Biologicals Cat#: 181
Luxol fast blue	Sigma	Sigma Cat#:L0294
Collagenase IV	Sigma	Sigma Cat#:C5138-500MG
Collagenase D	Roche	Roche Cat#: 11088866001
DNAse I	Sigma	Sigma Cat#:11284932001
Percoll	Fisher Scientific	Fisher Scientific Cat#: 45-001-747
FBS	Corning	Corning Cat#: 35-077-CV
EDTA	Bioshop	Bioshop Cat#:EDT111.500
HBSS	Thermo FisherScientific	Thermo FisherScientific Cat#: 14025092
Foxp3/Transcription Factor Staining Buffer Set	Thermo FisherScientific	Thermo FisherScientific Cat#: 00-5523-00
Fixable Viability Dye eFluor 506	Thermo FisherScientific	Thermo FisherScientific Cat#: 65-0866-18
phorbol 12-myristate 13-acetate (PMA)	Thermo FisherScientific	Thermo FisherScientific Cat#: J63916MCR
Ionomycin, Calcium Salt	Thermo FisherScientific	Thermo FisherScientific Cat#: I24222
OneComp eBeads Compensation Beads	Thermo FisherScientific	Thermo FisherScientific Cat#: 01-1111-42
[^{3}H]-thymidine	Perkin Elmer	Perkin Elmer Cat#: NET027A001MC
RNAlater	Thermo FisherScientific	Thermo FisherScientific Cat#: AM7024
GolgiPlug	BD	BD Cat#: 555029

(*Continued on next page*)

Please cite this article in press as: Cordeiro et al., Obesity intensifies sex-specific interferon signaling to selectively worsen central nervous system autoimmunity in females, Cell Metabolism (2024), https://doi.org/10.1016/j.cmet.2024.07.017

Continued

REAGENT or RESOURCE	SOURCE	IDENTIFIER
GolgiStop	BD	BD Cat#: 554724
L-glutamine	BioShop	Wisent Cat#: GLU999
Penicillin/Streptomycin	BioShop	BioShop Cat#: PST999.100
Sodium Pyruvate	Thermo FisherScientific	Thermo FisherScientific Cat#: 11360-070
MEM NEAA	Thermo FisherScientific	Thermo FisherScientific Cat#: 11140-050
RPMI 1640	Corning	Corning Cat#:10-041-CV
Critical commercial assays		
Olink Explore 1536	Olink Proteomics	OLink Proteomics Cat#: 1536
RNeasy Mini Kit	QIAGEN	QIAGEN Cat#: 74104
EasySep Mouse $CD4^+$ T Cell Isolation Kit	Stemcell	Stemcell Cat#: 19852
EasySep Mouse Naive $CD4^+$ T Cell Isolation Kit	Stemcell	Stemcell Cat#: 19765
MagniSort Mouse CD11c Positive Selection Kit	Thermofisher	Thermofisher Cat#: 8802-6861-74
SuperScript III reverse transcriptase	Thermofisher	Thermofisher Cat#: 18080093
Universal SYBR Green Master Mix	Thermofisher	Thermofisher Cat#: 4309155
GeneChip Mouse Gene 2.0 ST array	Thermofisher (Affymetrix)	Thermofisher Cat#: 902500
DNeasy PowerSoil Pro kit	QIAGEN	QIAGEN Cat#: 47014
VeriKine-HS Mouse IFN-α All Subtype ELISA kit	PBL Assay Science	PBL Assay Science Cat #:42115
VeriKine-HS Mouse IFN-β ELISA kit	PBL Assay Science	PBL Assay Science Cat #: 42410-1
Mouse Adipokine magnetic bead panel	Millipore	Millipore Cat#: MADKMAG-71K; RRID: AB_2801416
DAPI	Biolegend	Biolegend Cat#: 422801
Soluble anti-CD3e	Invitrogen	Invitrogen Cat#: 145-2C11
BD perm wash	BD	BD Cat#: 554723
X-Vivo 15 Serum Free Medium with Gentamicin and Phenol Red	Lonza	Lonza Cat#: 04-418Q
Dynabeads Human T-Activator CD3/CD28 for T Cell Expansion and Activation	Gibco	Gibco Cat#: 11131D; RRID: AB_2916088
mouse recombinant IL-12p70	Biolegend	Biolegend Cat#: 577004
mouse recombinant IFNγ	Biolegend	Biolegend Cat#: 575304
Human IL-17A ELISA Ready-set-go	Invitrogen	Invitrogen Cat#: 5017243
Human IFN-γ ELISA Ready-set-go	Invitrogen	Invitrogen Cat#: 5017325
Human IL-2 ELISA Ready-set-go	Invitrogen	Invitrogen Cat#: 14-7029-68
Mouse IL-17A ELISA MAX	Biolegend	Biolegend Cat#: 79108
Mouse IFN-γ ELISA OptEIA	BD	BD Cat#: 51-26121E
Mouse IL-2 ELISA	Invitrogen	Invitrogen Cat#: 14-7022-85
Mouse Flow Cytomix assays	Biolegend	Biolegend Cat#: BMS822FF
Deposited data		
Raw and processed microarray data	Geo	GEO: GSE241044
Olink data	Mendeley Data	Mendeley Data: https://doi.org/10.17632/44khystv6t.1
Experimental models: Organisms/strains		
C57BL/6J (#664)	The Jackson Laboratory	The Jackson Laboratory Cat#: RRID: IMSR_JAX:000664
SJL/J (#686)	The Jackson Laboratory	The Jackson Laboratory Cat#: RRID: IMSR_JAX:000686
C57BL/6-Tg (Tcra2D2,Tcrb2D2)1Kuch/J (#6912)	The Jackson Laboratory	The Jackson Laboratory Cat#: RRID: IMSR_JAX:006912

(*Continued on next page*)

Please cite this article in press as: Cordeiro et al., Obesity intensifies sex-specific interferon signaling to selectively worsen central nervous system autoimmunity in females, Cell Metabolism (2024), https://doi.org/10.1016/j.cmet.2024.07.017

CellPress
OPEN ACCESS

Continued

REAGENT or RESOURCE	SOURCE	IDENTIFIER
B6.129S2-Cd4tm1Mak/J (CD4 KO) (#2663)	The Jackson Laboratory	The Jackson Laboratory Cat#: RRID: IMSR_JAX:002663
B6.BKS(D)-Leprdb/(#697)	The Jackson Laboratory	The Jackson Laboratory Cat#: RRID: IMSR_JAX:000697
B6.Cg-Tg(Lck-icre) 3779Nik/J (#12837)	The Jackson Laboratory	The Jackson Laboratory Cat#: RRID: MGI:4442208
B6.129P2-Leprtm1Rck/J (#8327)	The Jackson Laboratory	The Jackson Laboratory Cat#: RRID: IMSR_JAX:008327
B6(Cg)-Ifnar1tm1.1Ees/J (#28256)	The Jackson Laboratory	The Jackson Laboratory Cat#: RRID: IMSR_JAX:028256
Oligonucleotides		
Ifng (FWD) 5' –TGGCTCTGCAG GATTTTCATG-3'	IDT	N/A
Ifng (REV) 5'- TCAAGTGGCATAGA TGTGGAAGAA3'	IDT	N/A
Stat1 (FWD) 5'-GGAGGTGAACC TGACTTCCA-3'	IDT	N/A
Stat1 (REV) 5'- TCTGGTGCTTCC TTTGGTCT-3'	IDT	N/A
Stat4 (FWD) 5'-TCTGCTCAAAGA TAAAATGCCTG-3'	IDT	N/A
Stat4 (REV) 5'-TCCATTTTCAGA TTGGTCCAC-3'	IDT	N/A
Tbx21 (FWD) 5'-GCCAAAGGATT CCGGGAGAA-3'	IDT	N/A
Tbx21 (REV) 5'-GGTAGAAACGG CTGGGAACA-3'	IDT	N/A
Actb (FWD) 5'-GAACCCTAAGG CCAACCG-3'	IDT	N/A
Actb (REV) 5'-CACGCACGATT TCCCTCT-3'.	IDT	N/A
Ifnar1 (FWD) 5'- AGAGGTAGTCTCC AGCTCCG-3'	IDT	N/A
Ifnar1 (REV) 5'- CGCCTCGTCTTT TGTTCGAT-3'	IDT	N/A
Leprb (FWD) 5'- ACAATTGTAAGAGA GGCTGCTGA-3'	IDT	N/A
Leprb (REV) 5'- AGGTGAACTCCAGTCACTCC-3'	IDT	N/A
Software and algorithms		
GraphPad Prism v9.5.0	GraphPad	RRID: SCR_002798
R v4.2.3	R	RRID: SCR_001905
Ingenuity Pathway Analysis (IPA)	QIAGEN	RRID: SCR_008653
FlowJo v10.8.1	TreeStar	RRID: SCR_008520
ImageJ	NIH	RRID: SCR_003070
GeneSpring software v12.1	Agilent	RRID: SCR_010972
DAVID Functional Annotation tool v6.8	NIH	RRID: SCR_001881
Qiime2 analysis package v2023.2	Qiime2	RRID: SCR_021258
Other		
High-fat diet (60% kcal of fat)	Research Diets	Research Diets Cat#: D12492i
Normal Chow Diet	Inotiv	# 7912

Please cite this article in press as: Cordeiro et al., Obesity intensifies sex-specific interferon signaling to selectively worsen central nervous system autoimmunity in females, Cell Metabolism (2024), https://doi.org/10.1016/j.cmet.2024.07.017

RESOURCE AVAILABILITY

Lead contact

Further information about requests for reagents and resources should be directed to the lead contact Shannon E. Dunn, shannon.dunn@utoronto.ca.

Materials availability

This study did not generate new unique reagents.

Data and code availability

- Raw and processed microarray data have been deposited in GEO: GSE241044. OLINK data was deposited in Mendeley Data: https://doi.org/10.17632/44khystv6t.1.
- This paper does not report original code.
- Data S1 contains the raw data values that were used to create all graphs in the paper. Additional information about research reagents is available in the key resources table.

EXPERIMENTAL MODEL AND SUBJECT DETAILS

Human subjects

For the OLINK analysis, 114 untreated RRMS patients and 45 healthy volunteers were consented to provide demographic information and serum between December 2012 to April 2021 (Table S1). Data pertaining to disease diagnosis, disease status, body mass index, and medication usage was extracted from medical records. Ethnicity, race, and sex were self-reported by the participants. RRMS patients were diagnosed using the 2010 or 2017 revised McDonald criteria.[71,72] RRMS patients who were not treatment-naive were off therapy for at least 1 month prior to the blood draw, with a median time off therapy of 4 months (range of 1-96 months). Written informed consent was obtained under an approved REB (IRB# 16-05) from individuals prior to participation in the study.

For experiments that examined the responses of human naive $CD4^+$ T cells to anti-CD3/anti-CD28, blood samples were drawn from individuals who self-identified as being healthy male and females (aged 20–30 years) after obtaining informed consent under an approved REB (REB 09-0577-AE) or IRB (IRB# 97959). All participants were free of medications with the exception of oral contraceptives, which were used by ~50% of the women. Other exclusion criteria included smoking and drug use, recent infection ($\leq$ 4 weeks), recent history of acute or history of chronic disease, or obesity (BMI $\geq$ 30 kg/m^2). Blood was collected from women during the self-reported follicular phase of the menstrual cycle. Blood draws were conducted in the morning hours.

Mouse model details and animal ethics

C57BL/6J (#664), SJL/J (#686), and B6.BKS(D)-*Lepr*^{db}/J (#697) (db/db mice) were obtained directly from Jackson Laboratory (Bar Harbor, ME, USA) and used for experiments. Breeder pairs of C57BL/6-Tg (Tcra2D2,Tcrb2D2)1Kuch/J (2D2) (#6912), B6.129S2-*Cd4*$^{tm1Mak/J}$ (CD4 KO) (#2663), B6.Cg-Tg(Lck-icre) 3779Nik/J (distal Lck-cre) (#12837), and B6.129P2-*Lepr*^{tm1Rck}/J (#8327), and B6(Cg)-*Ifnar1*$^{tm1.1Ees}$/J (#28256) were obtained from Jackson laboratory and were used to establish in-house colonies.

T cell-specific leptin receptor-deficient mice were generated by crossing mice that have a floxed first exon of the leptin receptor (#8327) with mice expressing Cre recombinase under the control of the distal Lck Cre promoter (#12837).[73] T cell-specific type I IFN receptor 1 (IFNAR1) mice were generated by crossing these Lck-Cre mice with mice bearing a floxed exon 3 of the IFNAR1 gene (#28256). F1 generation mice from either of these crosses were bred together to generate mice that were homozygotes for the floxed allele and either negative or heterozygotes for the Lck-Cre distal allele. F2 mice generated from these F1 pairings were bred together to generate littermates having these same genotypes for experiments.

$CD4^+$ T cell-specific leptin receptor-deficient mice were generated using a radiation bone marrow chimera (BMC) approach. For this procedure, BM cells were isolated from the tibias and femurs of 8–12 week old CD4 knockout, db/db, and C57BL/6J mice as described previously.[74] Briefly, femurs and tibias are removed and placed in 70% ethanol in a sterile petri dish for 2 minutes. This was followed by two washes (2 min each) in ice-cold sterile 1 x PBS. Bones were then cut at both ends using scissors and the bone marrow was then flushed out of the bones into a sterile petri dish using a 27-gauge needle syringe filled with 1 x PBS. Cells were dissociated through a 70 μm sieve, transferred to a 50 mL conical tube and then centrifuged (300 x g for 10 min). Red blood cells were lysed with by resuspending the cell pellet in 2 mL of Ammonium-Chloride-Potassium (ACK) lysis buffer (0.15 M NH_4Cl, 10 mM $KHCO_3$, 0.1 mM Na_2EDTA). The lysis reaction was stopped after 1 min and 15 s by adding excess 1 x PBS to the tube. Cells were centrifuged again and the pellet was resuspended in 1 x PBS and cells were counted using a hemacytometer and kept on ice until transfer.

Recipient CD4 KO mice (aged 7-9 weeks old) were lethally-irradiated with two 5.5 Gy doses of γ-irradiation, separated by a 3 h interval in a ventilated ^{137}Cs irradiator (MDS Nordion Gammacell 40). Irradiated CD4 KO recipient mice were injected i.v. via tail vein with 3-4×10^6 mixed BM donor cells of 80% CD4 knockout and 20% WT or 80% CD4 knockout and 20% db/db. Recipient mice were treated with 0.25 mg/ml Enrofloxacin containing water (Baytril NR, Bayer) for first 12 days following irradiation to prevent

Please cite this article in press as: Cordeiro et al., Obesity intensifies sex-specific interferon signaling to selectively worsen central nervous system autoimmunity in females, Cell Metabolism (2024), https://doi.org/10.1016/j.cmet.2024.07.017

infection. BMC mice were provided NCD or HFD for 4 weeks, starting at 8 weeks post-immune reconstitution. The reconstitution of $CD4^+$ T cells was verified by evaluating the percentage of $CD4^+$ T cells in heparinized peripheral blood, after red blood cell lysis, by flow cytometry using anti-CD4-FITC and CD3-APC antibodies.

All mice were maintained group-housed in a specific pathogen-free environment under 12 h: 12 h dark-light cycle. The temperature in the room where the animals were housed was monitored over a month period and was found to fluctuate between 19.6 and 20.3 °C. All experiments were conducted following the guidelines of the Canadian Council of Animal Care) under animal protocols (AUP 5937 and 153) that were approved by the University Health Network and St. Michael's hospital animal care committees.

Dietary treatments

In all experiments, mice were weaned to NCD consisting of 17% kcal of fat (7912, Harlan). For HFD studies, mice were either continued on NCD or switched to high-fat diet (HFD) consisting of 60% kcal of fat (D12492i, Research Diets). These diets were continued for 4-8 weeks depending on the experiment. Mice were weighed weekly. For the diet-reversal studies, mice that received HFD were switched back to NCD at 10 weeks of age.

Post-natal overnutrition model

Timed pregnancies were set up in female and male C57BL/6J mice that were set up in harems of two females with one male. Mice were bred together for four days before males were removed. Dams were kept on a breeding chow (Teklad Global 19% Protein Extruded Rodent Diet) throughout the pregnancy and lactation periods. Litters born within 72 h of one another were individually sexed and then pooled together with same-sex pups in one large cage. Pups were then randomly redistributed back to lactating dams to create sex matched litters of n = 3 pups/dam or n = 8 pups/dam. Pups were weighed weekly and weaned onto normal chow diet at postnatal day 24. Mice were 8 weeks of age at the time experiments were initiated or performed.

Ovariectomies

Female C57BL/6J mice, received from Jackson Laboratories aged 3 weeks were acclimatized for one week in the animal facility. At 4 weeks of age, mice were provided a bilateral ovariectomy or sham surgery. For ovariectomies, mice were anaesthetized with isoflurane and the skin was disinfected on the animals' back. A 1 cm incision was made in the skin on the animal's back just below the apex in the spine using sterile surgical scissors. Then, a 0.75 cm incision was made in the body wall on either side of the spine using fine scissors. Sterile forceps were used to grasp and externalize the abdominal fat pad (to which the ovary is attached). Fine scissors were used to sever the ovary at the juncture with the fallopian tube, and the fat pad was returned to the body cavity. Incisions were closed with 4-0 absorbable suture and the skin incision was closed with staples. For sham surgeries, the procedures were the same except that the ovary was not severed. Animals recovered two weeks before starting HFD, and six weeks prior to conducting immune studies at 10 weeks of age.

METHOD DETAILS

Human Blood Collection and Processing

For OLINK analysis, serum samples were collected in BD Vacutainer Serum tubes. Blood was allowed to clot for 60 minutes and then centrifuged at 1300 x g for 10 minutes. Serum was then aliquoted into tubes for storage at -80°C. For naive $CD4^+$ T cell studies, peripheral blood was collected in BD Vacutainer tubes with sodium heparin. Peripheral blood mononuclear cells (PBMCs) were isolated from heparinized blood using Ficoll-Paque density gradient centrifugation (GE Healthcare). Cells were washed in 1 x MACS buffer and were counted.

Proteomic Analysis on Human Serum

Proteins were measured from serum samples using Olink Explore 1536 from Olink Proteomics which combines the proximity extension assay (PEA)[75] with next-generation sequencing (NGS) technology.[76] The complete library contains antibodies targeting 1472 proteins, of which 1463 are unique proteins. Patient samples were randomized and incubated overnight with antibodies conjugated to oligonucleotide PEA probes at 4°C. After antibody binding, oligonucleotide annealing, and extension steps, the preamplification mix was added to the samples at room temperature. PCR amplification was performed, and PCR amplicons were then pooled and subjected to another PCR amplification step after addition of individual sample index sequences. After pooling of the samples, bead purification and quality control of the generated libraries were performed. Sequencing was carried out using Illumina's NovaSeq 6000 instrument. Quality control and normalization processes were then performed to translate barcode sequence counts into normalized protein expression (NPX) units. Assays on the samples were performed blinded from the clinical data. Significant differences in individual protein levels (NPX units) between obese and non-obese was determined using T tests (two groups were compared) and adjusted for multiple comparisons by the Bonferroni and Hochberg method (R v4.2.3). Statistical comparisons of individual proteins between three or more groups were determined using one-way ANOVA (GraphPad Prism v9.5.0). For bioinformatic analysis, differentially abundant serum proteins were mapped to biological pathways using Ingenuity Pathway Analysis (IPA) (QIAGEN Inc.).[77]

Please cite this article in press as: Cordeiro et al., Obesity intensifies sex-specific interferon signaling to selectively worsen central nervous system autoimmunity in females, Cell Metabolism (2024), https://doi.org/10.1016/j.cmet.2024.07.017

Genotyping

Mice positive for the 2D2 transgene (#6912) were identified as having a majority (>75%) of $CD4^+$ T cells that were double positive for Vβ11 and CD4 in peripheral blood. Staining of heparinized blood cells with CD4-FITC (GK1.5) and Vβ11-PE (RR3-15) antibodies (Biolegend) was performed as described previously.[78] In brief, a drop of blood was collected from the saphenous vein of mice into a FACS tube that contained 15 μl of 1 x PBS and 5 U/ml of heparin (Sigma). Cells were stained by adding 20 μl of FACS buffer (1 x PBS containing 2% fetal calf serum) containing the FITC-CD4 and Vβ11-PE antibodies directly to the tube containing blood. Tubes were incubated at room temperature in the dark for 30 min. Red blood cells were lysed via the addition of 2 mL of ACK lysis buffer to each tube. Once the cell suspension became transparent, 2 ml of FACS buffer was added to stop the cell lysis. Cells were centrifuged at 335 x g at 4°C for 5 min, the supernatant was decanted and cells were resuspended in FACS buffer for analysis. Genotyping of other mice was performed by PCR amplification of genomic DNA obtained from tail or ear snips according to the genotyping protocols provided by the Jackson Laboratory.

Fat mass and metabolic measurements

The inguinal fat pad (subcutaneous fat) and the gonadal fat pad (visceral fat) were dissected from mice and weighed. For glucose tolerance tests, mice were fasted overnight for 16 hours prior and then injected i.p. with 1 g/ kg of body weight of D-Glucose (Sigma) in 1 x PBS. Blood was collected by tail vein at 0, 15, 30, 60, 90, and 120 min post-injection using the Contour Next EZ glucometer (Bayer). For insulin tolerance tests, mice were fasted for 6 hours and then injected i.p. with 0.5 U/kg of body weight with human insulin (Humalog, Eli Lilly). Blood glucose levels were measured at 0, 15, 30, 24, 60, 90, and 120 min using the Contour Next EZ glucometer.

Active EAE Induction and immunization to assess the myelin-specific recall T cell response

Mice were injected subcutaneously on the left and right sides of the chest with 50 μl of emulsion/side containing either 100 μg MOG_{35-55} or $PLP_{139-151}$ (Genemed Synthesis) in complete Freund's adjuvant (CFA) that contained pestle-ground 2 mg/ml heat-killed *Mycobacterium tuberculosis* H37Ra in incomplete Freund's adjuvant (Difco Laboratories). For EAE induction in C57BL/6J mice, mice were provided 100-200 ng *Bordetella pertussis* toxin (PTX) (List Biologicals) i.p. on day 0 and day 2 post-injection. Each new lot of PTX was titrated in preliminary EAE studies prior for use in experiments. Mice were weighed and examined daily for development of clinical symptoms using a 5-point scale: 0= no clinical symptoms, 1= complete loss of tail tone, 2= hindlimb or foot weakness, 3= complete hindlimb paralysis in one or both limbs, 4= complete hindlimb paralysis and forelimb weakness and 5= death or moribund.

Percent demyelination in spinal cord white matter

At the endpoint of EAE, spinal cords were harvested from mice and were fixed in 10% formalin for 6 days and were embedded in a single paraffin block (~10-12 spinal cord cross-sections and 6 brain coronal sections/block).[79] Sections were cut at 5 μm thickness and were stained with luxol fast blue (LFB) to visualize demyelinating lesions.[79] In brief, slides were de-paraffinized in xylene and then rehydrated by incubating in baths of 100% ethanol (2 x 5 min) and 95% ethanol (3 min). Slides were then transferred into a glass staining dish containing LFB solution (0.1% solvent blue 38 from Sigma and 0.25% glacial acetic acid in 95% ethanol). The staining dish was sealed with paraffin and sections were incubated overnight in a 56°C oven. The following morning, slides were transferred into a distilled water bath. Then the following cycle was performed until the grey matter was sufficiently de-blued: slides were dipped in 0.2% lithium chloride solution for 5 seconds, were incubated in three consecutive 70% ethanol baths (2 dips each), and then held in water and visualized using the microscope. Sections were then dehydrated by incubating in 95% ethanol (2 x 5 min) followed by 100% ethanol (2 x 5 min). Sections were cleared for 5 min in xylene and then cover-slipped using Permount.

Slides were then scanned and images of each spinal cord section were converted to TIFF images that were imported into ImageJ.[79] The percent area of white matter that was stained with myelin was calculated as previously described.[79] In brief, each image was opened and converted to a grey scale image and then thresholding was performed such that the overlay captured all of the dark (myelin-stained) regions. The polygon tool was used to outline the dorsal spinal cord white matter as well as the anterior-lateral-white matter region of each spinal cord section. The area fraction was measured using this ImageJ tool under the measurement menu. This value from the dorsal and ventral-lateral white matter areas was averaged to determine a percent staining value for each section and then this value was averaged across all sections for each mouse. The percent demyelination was estimated by subtracting the percent area staining from 100%.

Mononuclear cell isolation from the CNS, spleens, and lymph nodes

CNS mononuclear cell isolation was performed at 2–4 days after the onset of EAE as described previously.[75,80] In brief, mice were anaesthetized using isoflurane and were transcardially-perfused with 20 ml of 1 x PBS (Calcium, magnesium free, Gibco) containing 5 U/ml of heparin (Sigma). For each mouse, the spinal cord and cerebellum were harvested and were pooled together in a tube containing 1 x HBSS (Ca^{2+}/Mg^{2+} free) and FBS. Tissues were then transferred into a sterile petri dish containing 1.5 mL of 1 x HBSS and were scissor-minced. An equal volume of 2 x collagenase IV (600 U/mL stock, Sigma) was added to the tissue mixture along with 15 μl of DNAase (1000 U/ml stock). Tissues were digested for 30 minutes at 37°C. The digested tissue was dissociated through a 70 μm sieve and then transferred to a conical tube and centrifuged for 10 min at 4°C (754 x g). The pellet was

Please cite this article in press as: Cordeiro et al., Obesity intensifies sex-specific interferon signaling to selectively worsen central nervous system autoimmunity in females, Cell Metabolism (2024), https://doi.org/10.1016/j.cmet.2024.07.017

resuspended in 5 mL of 40% Percoll (GE Healthcare) and this was slowly layered onto 2.5 mL of 70% Percoll contained in a conical tube. The gradient was centrifuged at 800 x g for 30 min (no brake). The myelin debris was removed from the top of the layer and then mononuclear cells were collected from the 40%/70% interface using a pipette and transferred to a fresh tube. Cells were washed twice by topping up the tube with 1 x HBSS followed by centrifugation (10 min at 300 g at 4°C) and Percoll gradient (GE Healthcare).[75,80] Cells were then resuspended in 200 μl of 1 x FACS buffer (1 x PBS supplemented with 2% FBS and 0.5M EDTA) or Complete T cell media (CM) that consisted of RPMI 1640, 10% FBS (Hyclone), 1 mM sodium pyruvate, 2 mM L-glutamine, 0.1 mM non-essential amino acids, 100 U/ml penicillin/streptomycin, and 0.5 μM 2-mercaptoethanol all from (Gibco) and were counted.

Spleens and axillary and inguinal lymph nodes were harvested from mice and were processed into a single cell suspension in sterile 1 x PBS by smashing through 70 micron sieves using the back end of a sterile syringe. Cells were centrifuged for 1 x 10 min at 300 x g. Red blood cells were lysed by resuspending the cell pellet (1 ml/spleen or lymph node) using ACK lysis buffer. The lysis reaction was stopped after 1 min and 15 s by adding excess 1 x PBS to the tube. Cells were centrifuged again and the pellet was resuspended in FACS buffer or CM and cells were counted using a hemacytometer.

Examining MOG_{35-55}-specific-peripheral T cell responses and adoptive transfer EAE studies

At 9 days post-immunization with MOG_{35-55} (C57BL/6J) or $PLP_{139-151}$ (SJL/J) and CFA, mononuclear cells were isolated from the spleen and axillary and inguinal lymph nodes and were re-suspended in CM as described above. Cells were cultured at 0.5 x 10^6 cells/well in 200 μl CM that contained various concentrations of MOG_{35-55} or $PLP_{139-151}$ for 48-72 h at 37°C in a 5% CO_2 incubator. Cytokines were measured in culture supernatants using mouse Ready-Set-Go (Invitrogen) or Legend MaxTM kits (Biolegend) ELISA kits at the time of peak cytokine production: IFN-γ (at 48 or 72h), IL-17A (72 h), or IL-2 (24 or 48 h). Absorbance was read at 450 nm using a VictorX3 plate reader (Perkin Elmer).

For adoptive transfer EAE studies, spleen and lymph nodes from control or DIO C57BL/6J females or males were processed in a similar manner except that cells were plated at 4.0 x 10^6 cells/ml in CM in tissue culture-treated vented 75 cm^2 flasks in the presence of 10 μg/ml MOG_{35-55} and 10 ng/ml mouse recombinant IL-12p70 (Biolegend). After 72 h, non-adherent cells were collected from flasks, were washed three times in 1 x PBS (centrifuging between, 300 x g at 4°C) and then placed on ice. Thirty million cells were injected i.p. into each recipient male C57BL/6J mice.

Flow cytometry

Centrifugations were conducted at 300 x g for 5 min following each wash to pellet cells. Cells (1 x 10^6/stain) were washed twice in 1 x FACS buffer. Fc receptors were blocked by incubating cells with 0.5 μg purified CD16/CD32 (93) antibody (Biolegend) in 50 μl 1x PBS for 15 min at 4°C. Cells were washed with 1 x PBS, and then 1 x 10^6 cells were stained for 30 min at 4 °C with Fixable Viability Dye eFluor 506 (1:1000) (Thermo FisherScientific) and cell surface antibodies diluted in 100 μl FACS buffer for 30 min at 4°C. Antibodies include: APC-CD3 (145-2C11), FITC-CD3 (145-2C11), FITC-CD4 (GK1.5), PE-Cy7-CD4 (RM4-5), PE-Cy5-CD8 (53–6.7), PE-CD11b (M1/70), APC-CD11b (M1/70), APC-CD11c (HL3), BV421-CD19 (B4), PE-CD25 (PC61.5), APC-CD25 (PC61.5), FITC-CD44 (IM7), PE-CD44 (IM7), PE-Cy5-CD44 (IM7), PE-Cy7-CD44 (IM7), Alexa fluor700-CD44 (IM7), PE-Cy7 CD45 (30-F11), PE-CD45.1 (A20), PE-Cy7 CD45.1 (A20), FITC-CD45.2 (104), PE-IFNAR1 (MAR1-5A3), Biotin-IFNAR1 (MAR1-5A3), PE-IFNGR1 (GIR-208), eFluor450-IL-18Ra (P3TUNYA), FITC-Ly6G (1A8), PE-Vbeta11 TCR (RR3-15) and SB600-NK1.1 (PK136). Cell surface staining with Biotin-IFNAR1 was followed by a 20 minute incubation with Strepavidin-APC. Cells were washed twice with 1 x FACS buffer before proceeding to flow cytometry.

For intracellular cytokine staining, cells were stimulated with 10 ng/ml PMA and 750 nM Ionomycin in CM with GolgiPlug or GolgiStop for 3-6 hours at 37°C. Viability and cell surface antibody staining was performed as described above. Cells were fixed in 4% PFA (Electron Microscopy Sciences) for 10 min at RT and were washed twice in FACS buffer and then incubated in 1x Perm/Wash buffer (BD) for 15 min at 4°C. After centrifugation, cells were stained with cytokine antibodies diluted in 1x Perm/Wash buffer for 30-60 min at 4°C. After two washes in 1x Perm/Wash buffer, cells were resuspended in FACS buffer for acquisition. Alternatively, cells were fixed and permeabilized and cytokine and FoxP3 staining was performed using reagents and instructions provided with the Foxp3/Transcription Factor Staining Buffer Set (Thermo Fisher Scientific). Antibodies used for intracellular and intranuclear staining include: PE-FOXP3 (FJK-16s), Alexa488-FOXP3 (MF-14), FITC-GM-CSF (MP1-22E9), PE- IFN-γ (XMG1.2), APC-IFN-γ (XMG1.2), APC-IL-17A (eBio17B7) and PE-IL-17A (eBio17B7).

For MOG tetramer staining, Fc receptors were blocked, and cells were incubated with the mouse IA^b-MOG_{38-49} variant S45D or IA^b-human $CLIP_{87-101}$ tetramer-APC reagents (NIH Tetramer Core Facility at Emory University) for 3 h at 37°C at 1:50 dilution in 50 μl of T cell complete media. After washing in 1 x PBS, samples were stained with CD4-PE-Cy7, CD44-FITC, and Fixable Viability Dye eFluor 506 for 30 min at 4°C, and washed again with 1 x FACS buffer prior to flow cytometry.

For assessment of phospho-STAT (Y701) and total STAT staining, 10^6 cells were plated, stimulated, fixed, and permeabilized in the same 96-well U-bottomed plate. Cells were first serum-starved at 37°C for 1 h in RPMI prior to stimulation. eFluor 506 viability dye (prepared in 1 x PBS) was added to wells in the last 15 minutes of incubation. Cells were then stimulated with 100 ng/ml recombinant mouse IFN-γ (100 ng/ml) (Invitrogen) at 37°C. Stimulations were stopped by adding PFA (1.5% final concentration) to the wells at 0, 2, 5, 10 min, 15 min. For total STAT1 intracellular staining, cells were instead stained with viability dye (1:1000 in 1 x PBS) and then were fixed in 1.5% PFA. For both phospho-STAT and total STAT staining workflows, post-PFA-fixation, cells were permeabilized with ice-cold methanol (pre-chilled at -20°C, Fisher Scientific) for 10 min on ice and then were washed twice with 1 x PBS. Fc receptor

Please cite this article in press as: Cordeiro et al., Obesity intensifies sex-specific interferon signaling to selectively worsen central nervous system autoimmunity in females, Cell Metabolism (2024), https://doi.org/10.1016/j.cmet.2024.07.017

blockade was performed as described above and cells were then stained in 1 x FACS buffer for 1 h at RT with both cell surface- and intracellular-targeted antibodies: anti-Stat1 pY701-Alex Fluor 647 (4a), CD4-APC-eF780 (GK1.5), CD44-PE (IM7), CD8-FITC (53-6.7), and CD19-BV421 (B4) for IFN-γ signaling and Stat1 (N-Terminus)-Alexa Fluor 647 (1/STAT1), CD4-APC-eF780 (GK 1.5), CD44-PE (IM7), CD8-FITC (53-6.7), and CD19-BV421 (B4) in FACS for STAT1 expression. Cells were washed twice in 1 x FACS buffer, and were resuspended in 1 x FACS buffer for acquisition.

Cells were acquired either on an LSR II (BD Biosciences) or Sony SP6800 and were analyzed using FlowJo (TreeStar). OneComp eBeads Compensation Beads (Invitrogen) were used as single stain controls. Fluorescence minus one (FMO) controls or unstimulated controls were used to set gates.

Dendritic cell (DC)/CD4$^+$ T cell co-culture assay

For dendritic cell isolation studies, spleens were harvested from mice and then were placed in a petri dish containing 1 x HBSS (Gibco) supplemented with 1 mg/ml collagenase D (Roche). The tissue was injected with the collagenase D in 1 x PBS using 27 G needle and syringe and then the tissue was digested for 30 min at 37°C. Digested tissue was then dissociated through a 70 μm cell strainer into 1 x PBS. Cells were centrifuged, red blood cells were lysed in ACK lysis buffer, and cells were washed and resuspended in 1 x MACS buffer. CD11c$^+$ cells were isolated from spleen mononuclear cells using the CD11c$^+$ Magnisort kit (Invitrogen) and were resuspended in CM. These cells were irradiated at 30 Gy using a Cesium irradiator, were washed, and resuspended in CM. Total CD4$^+$ T cells from 2D2 mice were negatively selected using magnetic isolation kits (Stem Cell or Invitrogen). In brief, spleens and lymph nodes from 2D2 mice were dissected, mononuclear cells were isolated and red blood cells lysed as described above, and cells were resuspended in 1 x MACS buffer. Magnetic isolation was performed according to kit directions and cells were resuspended in CM for counting. CD4$^+$ T cells were co-cultured together with CD11c$^+$ cells (1:2 ratio) with 0, 5, 20, or 40 μg/ml MOG_{35-55}. The proliferation of CD4$^+$ T cells was measured by [^{3}H]-thymidine incorporation assay (wells pulsed 48 h and cells harvested 18 h later). Cytokine levels were measured in culture supernatants at 48 h using Ready-set-go ELISA kits (Invitrogen).

Treg suppression assay

CD4$^+$ T cells from either DIO or NCD-fed mice magnetically isolated by negative selection from spleens and lymph nodes and then cells were stained for antibodies specific against CD4, CD25, CD44, and DAPI. CD4$^+$CD25$^+$ Tregs and CD4$^+$CD44$^{low\text{-}int}$ CD25$^-$ naive T cells were FACS using an Aria II FACS Sorter (BD) at the Sickkids/UHN flow cytometry facility. Cell fractions were washed, counted, and resuspended in CM. Tregs from DIO and control mice were co-cultured with CD4$^+$CD44$^{low\text{-}int}$ T cells from sex-matched NCD-fed mice at the indicated ratios together with irradiated (30 Gy) splenocytes from sex-matched control mice and 5 μg/ml of soluble anti-CD3e (145-2C11) (Invitrogen). Cells were pulsed with by [^{3}H]-thymidine at 72 h and cells were harvested 18 h later and beta counting (in CPM) was performed as described below.

[^{3}H]-Thymidine incorporation assay

Cells were pulsed with thymidine (0.5 μCi/well) (Perkin Elmer). Eighteen hours later, cells were harvested onto glass fiber filter paper (Brandel Scientific) using a PHD cell harvester (Cambridge Technologies). Filter paper discs were air-dried overnight. The radioactivity in counts per minute (CPM) in filter paper discs was measured in liquid scintillation cocktail (MP Biomedicals) using a beta counter (Perkin Elmer). In all cases, the peak in the T cell proliferative response is shown.

Murine and human naive CD4$^+$ T cell stimulation assays

For mice, naive CD4$^+$CD44^{lo} T cells from spleen and lymph node mononuclear cell populations were resuspended in MACS buffer (Miltenyi) and further isolated by negative selection according to kit directions (Miltenyi) or by FACS sorting after cell surface staining with CD3 and CD44 antibodies using a FACS Aria II (Sickkids Flow Cytometry facility). For bead isolation, the purity of isolated CD4$^+$ T cells was >95% as verified by flow cytometry using anti-CD4 and anti-CD44 antibodies. Post-isolation, cells were washed twice in CM and then plated on plates that had been pre-coated with 0-5 μg/ml of CD3 and CD28 antibodies.

Human naive CD4$^+$ T cell stimulations were performed as described previously in X-VIVO media-15 with Dynabeads human T-activator anti-CD3 and anti-CD28 (1 bead for every 5 cell).[47] Proliferation of cells was measured by [^{3}H]-thymidine incorporation assay in CPM. Cytokines were measured in the culture supernatants by ELISA using Ready-Set-Go human IL-2, IFN-γ, IL-17 ELISA kits (Invitrogen). Measurements shown were sampled in the linear phase of the activation curve.

Real-time RT-PCR

Naive CD4$^+$ T cells were isolated spleens and lymph nodes of female and male control or DIO mice and were frozen. Alternatively, naive CD4$^+$ T cells were isolated as described above and stimulated with 2 μg/ml of plate-bound anti-CD3e and anti-CD28 (Invitrogen) for 0, 4, 8, and 16 h. Total RNA was isolated using a RNeasy Mini Kit (Qiagen) and RNA concentration and purity were measured using a NanoDrop (Thermo Fisher). cDNA was generated by reverse-transcribing 100 ng total RNA using SuperScript III reverse transcriptase (Invitrogen). For real-time PCR (qPCR), cDNA amplification was performed using Universal SYBR Green Master Mix

Please cite this article in press as: Cordeiro et al., Obesity intensifies sex-specific interferon signaling to selectively worsen central nervous system autoimmunity in females, Cell Metabolism (2024), https://doi.org/10.1016/j.cmet.2024.07.017

CellPress
OPEN ACCESS

(Roche) following the manufacturer's instructions. Data was normalized to *ActB*. Relative fold change was calculated using the Livak-method. Primers sequences are listed in the key resources table.

Microarray

Naive CD4$^+$ T cells (CD4$^+$ CD44$^{ow\text{-}int}$) were magnetically isolated by negative selection from spleens and lymph nodes and either immediately frozen or stimulated with 2 μg/ml plate-bound anti-CD3 and anti-CD28 antibodies for 16 h as described above. Total RNA was isolated using the RNEAsy kit (Qiagen). Total RNA quality was verified using the RNA 6000 Pico LabChip on a 2100 BioAnalyzer (Agilent). Ten ng of total RNA was reverse transcribed using GeneChip WT Pico Kit (Affymetrix). Each sample was hybridized to a GeneChip Mouse Gene 2.0 ST array (Affymetrix) for 16-18 h at 45°C. The arrays were scanned using a GeneChip Scanner 3000 (Affymetrix).

Data were analyzed using GeneSpring software (Version 12.1, Agilent) and was summarized using the ExonRMA16 algorithm followed by quantile normalization. A one-way ANOVA with post-hoc test (Tukey HSD test) and Benjamini-Hochberg FDR (false discovery rate) correction was used to identify differentially expressed genes ($p \leq 0.05$). The enrichment of functional categories was tested using Database for Annotation, Visualization and Integrated Discovery (DAVID) Functional Annotation tool v6.8. For this analysis, lists of positively or negatively regulated genes (fold change of 1.5 cut-off for stimulated CD4$^+$ T cells) were exported for use in DAVID. Each of these lists was analyzed against the background entities represented on the array. Gene ontology (GO) terms were compared using Benjamini-Hochberg FDR (false discovery rate) corrected p-values. The lists of differentially expressed genes were also compared against a published list of Th lineage genes[27] and were used to query the IMMGEN dataset of IFN-stimulated genes in CD4$^+$ T cells in the microarray browser to determine if they were inducible by type I, type II, or both type I and type II IFNs (http://immgen.org/ Skyline_microarray/skyline.html).

Fecal DNA extraction

Fecal pellets from mice were collected and immediately flash frozen in liquid nitrogen. DNA was then extracted using DNeasy PowerSoil Pro kit (Qiagen) following the manufacturer's instructions. Purity and quality of the DNA was assessed by NanoDrop (Thermo Scientific).

16S rRNA gene sequencing

The V4 hypervariable region of the 16S rRNA gene was amplified using uniquely barcoded 515F (forward) and 806R (reverse) sequencing primers to allow for multiplexing.[76] Amplification reactions were performed in a 25 μl reaction using 12.5 μL KAPA2G Robust HotStart ReadyMix (KAPA Biosystems), 1.5 μL each 10 μM forward and reverse primers, 7.5 μL of sterile water and 2 μL of DNA. The V4 region was amplified by cycling the reaction at 95°C for 3 minutes, 18 x cycles of 95°C for 15 seconds, 50°C for 15 seconds and 72°C for 15 seconds, followed by a 5-minute 72°C extension. Amplification reactions were done in duplicate to reduce amplification bias, were pooled, and amplicon lengths verified on 1% agarose TBE gels. Pooled duplicates were quantified using PicoGreen and combined by even concentrations. The library was then purified using Ampure XP beads and loaded on to the Illumina MiSeq for sequencing, according to manufacturer instructions (Illumina). Sequencing was performed using the V2 (150bp x 2) chemistry. A single-species (*Pseudomonas aeruginosa* DNA), a mock community (Zymo Microbial Community DNA Standard D6305), and a template-free negative control were included in the sequencing run. Sequencing was conducted at the Centre for the Analysis of Genome Evolution and Function (CAGEF) at the University of Toronto.

Analysis of the bacterial microbiome

The Qiime2 analysis package version 2023.2 was used for sequence analysis.[77] The quality of the sequencing run was first examined using FastQC. Cut adapt was used, following the default settings, to remove sequences with high error rates. Paired-end sequences were assembled, and quality trimmed using vsearch –fastq_mergepairs. The resulting high-quality data was then processed following the deblur pipeline. Sequences were clustered into Amplicon Sequence Variants (ASV) groups and singleton sequences were removed. Taxonomy assignment was executed using the Qiime2 classify-hybrid-vsearch-sklearn function and the Average ReadyToWear trained Silva database version 138.1. ASVs with an abundance less than 0.01% are removed to reduce the potential for observing bleed-through ASVs, and ASVs identified as contaminating chloroplast or mitochondria are removed. A phylogenetic tree was created using the SEPP function available through Qiime2.

Serum cytokine and chemokine measurements

Serum cytokine and chemokine levels were measured using a Mouse Adiponectin ELISA kit (Invitrogen), VeriKine-HS Mouse IFN-α All Subtype ELISA and Mouse IFN-β kit (PBL Assay Science), Mouse Adipokine magnetic bead panel (Millipore), and Mouse FlowCytomix assays (eBioscience, Invitrogen), following the manufacturer's protocols.

QUANTIFICATION AND STATISTICAL ANALYSIS

With the exception of microarray and microbiome analysis, data were analyzed with GraphPad Prism (v5). Data is represented as mean ± S.E.M, except where noted. Statistical significance was set at $p \leq 0.05$. A two-way ANOVA was performed followed by a

Please cite this article in press as: Cordeiro et al., Obesity intensifies sex-specific interferon signaling to selectively worsen central nervous system autoimmunity in females, Cell Metabolism (2024), https://doi.org/10.1016/j.cmet.2024.07.017

Bonferroni post-hoc test to examine diet by sex interactions, surgery by diet interactions, or diet by genotype interactions. Sample sizes ranged between n=3-8/group for most studies, a sample size where homogeneity of variance tests have low power. Thus for greater than 2 sample comparisons, a one-way ANOVA with Tukey post-hoc test was used when group variances appeared to be similar, whereas a Kruskal-Wallis test (> 3 groups) and a non-parametric post-hoc test were used when group variances appeared to be non-homogeneous. Unpaired two-tail Mann-Whitney U tests were used for two group comparisons with the exception of when sample sizes were two small (n=3/group) for this test to be valid. In this case, an unpaired two-tail T-test was used. Linear correlation was determined using non-parametric Spearman's test.